



Nitrogen- and irradiance-dependent variations of the maximum quantum yield of carbon fixation in eutrophic, mesotrophic and oligotrophic marine systems

MARCEL BABIN,* ANDRÉ MOREL,* HERVÉ CLAUSTRE,* ANNICK BRICAUD,* ZBIGNIEW KOLBER† and PAUL G. FALKOWSKI†

(Received 6 January 1995; in revised form 27 December 1995; accepted 4 January 1996)

Abstract—Natural variability of the maximum quantum yield of carbon fixation ($\phi_{C \max}$), as determined from the initial slope of the photosynthesis-irradiance curve and from light absorption measurements, was studied at three sites in the northeast tropical Atlantic representing typical eutrophic, mesotrophic and oligotrophic regimes. At the eutrophic and mesotrophic sites, where the mixed layer extended deeper than the euphotic layer, all photosynthetic parameters were nearly constant with depth, and $\phi_{C \max}$ averaged between 0.05 and 0.03 mol C (mol quanta absorbed)⁻¹, respectively. At the oligotrophic site, a deep chlorophyll maximum (DCM) existed and $\phi_{C \max}$ varied from *ca* 0.005 in the upper nutrient-depleted mixed layer to 0.063 below the DCM in stratified waters. Firstly, $\phi_{C \max}$ was found roughly to covary with nitrate concentration between sites and with depth at the oligotrophic site, and secondly, it was found to decrease with increasing relative concentrations of non-photosynthetic pigments. The extent of $\phi_{C \max}$ variations directly related to nitrate concentration was inferred from variations in the fraction of functional PS2 reaction centers (*f*), measured using fast repetition rate fluorometry. Covariations between *f* and nitrate concentration indicate that the latter factor may be responsible for a 2-fold variation in $\phi_{C \max}$. Moreover, partitioning light absorption between photosynthetic and non-photosynthetic pigments suggests that the variable contribution of the non-photosynthetic absorption may explain a 3-fold variation in $\phi_{C \max}$, as indicated by variations in the effective absorption cross-section of photosystem 2 (σ_{PS2}). Results confirm the role of nitrate in $\phi_{C \max}$ variation, and emphasize those of light and vertical mixing. Copyright © 1996 Elsevier Science Ltd

INTRODUCTION

The maximum quantum yield of photosynthesis is a critical variable in bio-optical models of primary productivity (Bannister, 1979; Kiefer and Mitchell, 1983; Sakshaug *et al.*, 1989; Smith *et al.*, 1989; Morel, 1991; Platt *et al.*, 1992; Bidigare *et al.*, 1992). In oxygenic photosynthesis, it is defined as the maximum rate of O₂ evolved or CO₂ fixed per mole absorbed photons (Kok *et al.*, 1970; Myers, 1980; Falkowski and Raven, *in press*). Although it sometimes is ecologically convenient to define an apparent quantum yield with reference to incident rather than absorbed light (Odum, 1971; Dubinsky and Berman, 1976; Dubinsky, 1980), the quantum yield relevant to bio-optical models is referenced to absorbed

* Laboratoire de Physique et Chimie Marines, Université Pierre et Marie Curie and CNRS, BP 8, F-06230, Villefranche-sur-Mer, France.

† Oceanographic and Atmospheric Sciences Division, Brookhaven National Laboratory, Upton, NY 11973, U.S.A.

light (Kok and Radmer, 1976). Hence, we adopt here the latter, biophysically more formal, definition.

For each molecule of O₂ evolved in the photosynthetic apparatus, two molecules of water are photochemically oxidized, leading to the production of four electrons and four protons. Each electron derived from water undergoes two photochemical reactions in series, and each of the photochemical reactions has a quantum yield of unity (Kok *et al.*, 1970). Therefore, for each molecule of O₂ evolved, a minimum of eight quanta were absorbed, giving a maximum quantum yield for oxygen evolution of 0.125 mol O₂ (mol quanta)⁻¹ (Kok, 1960). It should be noted that maximum yield for oxygen evolution is almost always greater than that for CO₂ fixation. Electrons derived from the photochemical oxidation of water are used to reduce nitrate and sulfate in addition to CO₂ (Myers, 1980; Ley and Mauzerall, 1982; Dubinsky *et al.*, 1986; Laws, 1991). Hence, it is commonly taken, based on experimental data, that the maximum quantum yield for carbon fixation is *ca* 0.08 mol CO₂ fixed per mol quanta absorbed (Myers, 1980; Bannister and Weidemann, 1984).

Biological oceanographers have often assumed that the maximum quantum yield is constant (Platt *et al.*, 1980; Kiefer and Mitchell, 1983; Kiefer *et al.*, 1989; Morel, 1991). This assumption has arisen from both mathematical convenience in parameterizing models and consideration of theoretical aspects of photosynthetic processes (Bannister, 1974; Bannister and Weidemann, 1984). It must be stressed, however, that the maximum achieved is, more often than not, lower than the maximum value recalled above (Myers, 1980). There are a number of potential reasons for a reduction in the maximum quantum yield. First, many photosynthetic organisms contain pigments that absorb photosynthetically available radiation (PAR) but do not transfer the absorbed excitation energy to a photochemical reaction center (Haxo and Blinks, 1950; Dubinsky *et al.*, 1986). Secondly, the number of photochemically competent reaction centers can vary as a function of irradiance (Neale, 1987; Vassiliev *et al.*, 1994; Olaizola *et al.*, 1994; Long *et al.*, 1994) or nutrient status (Welschmeyer and Lorenzen, 1981; Neale, 1987; Kolber *et al.*, 1988; Cleveland *et al.*, 1989; Herzig and Falkowski, 1989; Falkowski *et al.*, 1992; Falkowski, 1992; Greene *et al.*, 1994; Long *et al.*, 1994; Olaizola *et al.*, 1994; Vassiliev *et al.*, 1994). Third, cyclic electron flow around either photosystem 1 (PS1) (Slovacek *et al.*, 1980; Myers, 1987; Cha and Mauzerall, 1992) or photosystem 2 (PS2) (Heber *et al.*, 1979; Falkowski *et al.*, 1986a) permits photochemical utilization of absorbed excitation energy without concomitant production of O₂ or reduction of CO₂. Hence, it should not be surprising that the maximum quantum yields of photosynthesis observed in nature are lower than the theoretically achievable maximum (Bannister and Weidemann, 1984; Cleveland *et al.*, 1989; Babin *et al.*, 1995). What is unclear, however, is the extent of variability in the maximum quantum yield in the oceans and the causes of the variability.

Definitions and determinations of quantum yields

From a practical standpoint, oceanographers often determine photosynthesis as the rate of incorporation of radioactively labeled inorganic carbon into acid-stable particulate organic matter. If the exposure to the label is for a sufficiently short period, respiratory losses of radioactively labeled organic carbon are negligible and hence the rate of carbon incorporation is a reasonable measure of gross photosynthesis (Eppley and Sharp, 1975; Li and Goldman, 1981). The maximum quantum yield of carbon fixation, $\phi_{C \max}$, is calculated from:

$$\phi_{C \max} = \alpha^B / 12\,000 \bar{a}^* \quad (1)$$

where 12 000 is the molar weight (mg) of carbon, α^B [$\text{mg C (mg chl } a)^{-1}$ (mol available quanta $\text{m}^{-2})^{-1}$] is the chlorophyll-specific initial slope of the photosynthesis-irradiance curve (i.e. the “ P^B vs E ” curve) determined from incubation experiments, and \bar{a}^* is the mean chlorophyll-specific absorption coefficient of algae, weighted by the spectral distribution [$E(\lambda)$] of the photosynthetic available irradiance (from 400 to 700 nm; PAR) used during the experiment; the \bar{a}^* [m^2 (mg chl $a)^{-1}$] is calculated as:

$$\bar{a} = \int_{400}^{700} a_{\text{ph}}(\lambda) E(\lambda) d\lambda / \int_{400}^{700} E(\lambda) d\lambda \quad (2)$$

where $a_{\text{ph}}^*(\lambda)$ are the spectral values of the chlorophyll specific absorption coefficient of algae.

Calculations of $\phi_{C \max}$ for natural communities using Equations (1) and (2) have been reported by Cleveland *et al.* (1989; 14 values), Schofield *et al.* (1993; 64 values), Lizotte and Priscu (1994; 24 values), Marra and Bidigare (1994; 7 values) and Babin *et al.* (1995; 170 values). All five studies have revealed variability in $\phi_{C \max}$, although the causes of variability could not be unambiguously identified and understood.

An indirect way of determining a quantum yield of photosynthesis is based on measurements of variable fluorescence (Eppley and Sharp, 1975; Ley and Mauzerall, 1982; Falkowski and Kolber, 1993; Geider *et al.*, 1993; Kolber and Falkowski, 1993; Falkowski and Kolber, 1995). In this approach, active stimulated fluorescence techniques [“pump and probe” fluorometry or fast repetition rate fluorometry (FRR); e.g. Vassiliev *et al.*, 1994] are used to measure the variable component of fluorescence, quantitatively associated with photochemical efficiency of PS2. The principle is to measure the difference in fluorescence signal emitted *in vivo* by chl a in a dark-adapted condition, when all reaction centers are oxidized, F_o , and that obtained when all reaction centers are closed and fluorescence is maximal, F_m (Duysens and Sweers, 1963; Butler and Kitajima, 1975; Butler, 1978). The maximum quantum efficiency of photochemistry, denoted ϕ_{PS2} , is given by the ratio $(F_m - F_o)/F_m$; this yield should not be confused with the maximum quantum yield for oxygen evolution or carbon fixation. ϕ_{PS2} is directly related to the fraction of functional PS2 reaction centers, f . However, f is better expressed by (Falkowski *et al.*, 1986b; Kolber and Falkowski, 1993; Lavergne and Leci, 1993; Lavergne and Trissl, 1995; Kolber and Falkowski, 1992):

$$f = \frac{1}{8} \frac{F_m - F_o}{F_o} \quad (3)$$

where the factor 1.8 represents the maximum value for the ratio $(F_m - F_o)/F_o$ obtained in nutrient replete, exponential-phase laboratory cultures (Kolber *et al.*, 1988; see Appendix). By following the rate of change of the fluorescence signal as a function of the intensity of the actinic light, it is also possible to rapidly determine the effective absorption cross-section of PS2, σ_{PS2} [m^2 (quanta) $^{-1}$] (see later, equation (5)). Finally, the maximum quantum yield of carbon fixation, $\phi_{C \max}$, can be related to photosystem 2 characteristics through (see Kolber and Falkowski, 1993):

$$\phi_{C \max} = \frac{\sigma_{\text{PS2}} \phi_e f n_{\text{PS2}}}{\bar{a}^* R} \quad (4)$$

where n_{PS2} is the total number (functional and non-functional) of PS2 per unit of chl *a* [mol electron (mg chl *a*)⁻¹], ϕ_e is the quantum yield of electron transport for O₂ evolution [assumed to be 0.25 mol O₂ (mol electron)⁻¹], R is the photosynthetic quotient [mol O₂ (mol C)⁻¹], and \bar{a}^* is calculated from equation (2) using the spectral distribution of radiant energy [$E(\lambda)$] delivered by the probe flash.

Both the maximum quantum efficiency of photochemistry, ϕ_{PS2} , and the number of functional reaction centers (note that these are not independent variables) are markedly lower when algal cells are photoinhibited (Henley *et al.*, 1992; Long *et al.*, 1994; Vassiliev *et al.*, 1994). However, in addition, a hyperbolic relationship between between the maximum quantum efficiency of photochemistry and the rate of nitrogen supply has been observed in chemostat cultures (Kolber *et al.*, 1988), as well as in natural phytoplankton assemblages (Kolber *et al.*, 1990; Falkowski *et al.*, 1991; Geider *et al.*, 1993). Nitrogen limitation would induce losses of proteins involved in the structure of PS2 reaction centers and thereby depress f (Kolber *et al.*, 1988; Falkowski *et al.*, 1989).

The changes in fluorescence flash yields that are related to the photochemical reactions in PS2 can be observed only if light is absorbed by the reaction center. If excitation energy is absorbed by pigments that do not transfer the energy to PS2 reaction centers, and if the fraction of that transferred energy to the total absorbed energy is a variable, then the relationship between the maximum quantum efficiency of photochemistry and that for carbon fixation will be variable. The converse is not true however. All electrons that are used in the photosynthetic reduction of inorganic carbon originated from water and had to pass through PS2. Hence, all changes in f are directly reflected on $\phi_{\text{C max}}$ (expressed by equation (4)). Therefore, if f is sensitive to supraoptimal irradiance or nutrient supply, $\phi_{\text{C max}}$ would be similarly sensitive.

The first objective of the present study is to document variations in $\phi_{\text{C max}}$ in the ocean. To reach this objective, about 200 values of this maximum yield were determined in the northeast tropical Atlantic at three sites selected to represent typical EUtrophic, MEsotrophic and oLIgotrophic regimes (EUMELI/JGOFS-France Program). These measurements are *a priori* believed to reflect, in large part, the range of $\phi_{\text{C max}}$ natural variability, given the diversity encountered in terms of physical conditions (light and density vertical gradients), nutrient status and phytoplanktonic assemblages.

A second objective was to examine the sources of variability in $\phi_{\text{C max}}$. To accomplish this, we simultaneously monitored the changes in the fraction of functional PS2 reaction centers, f , using a Fast Repetition Rate fluorescence method (Kolber and Falkowski, 1992; Falkowski and Kolber, 1995) and compared these measurements with those obtained for $\phi_{\text{C max}}$. Our third objective was to assess the relative importance of nutrient deficiency, of the presence of non-photosynthetic pigments and of possible photodamage in determining the natural variations of $\phi_{\text{C max}}$. The simultaneous measurements of $\phi_{\text{C max}}$ and f , and the application of equation (4) are tentatively used to deconvolute these different effects.

MATERIAL AND METHODS

Eutrophic, mesotrophic and oligotrophic sites in the tropical northeast Atlantic (see legend of Fig. 1) were occupied for 3, 4 and 6 days during the EUMELI no. 4 cruise (June, 1992). Nutrients and pigments, optical properties, P^{B} vs E incubations and FRR fluorometry measurements were made daily. Sampling was generally performed at dawn, midday and dusk at 10 depths encompassing the whole algal vertical distribution. Samples

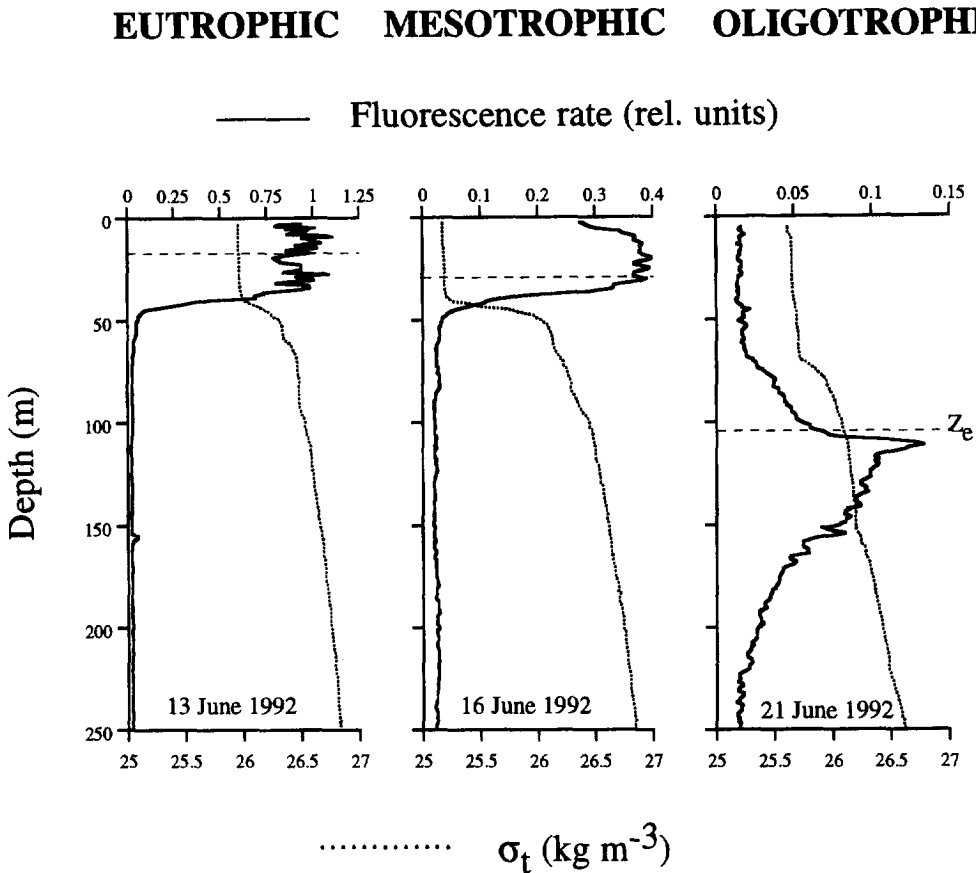


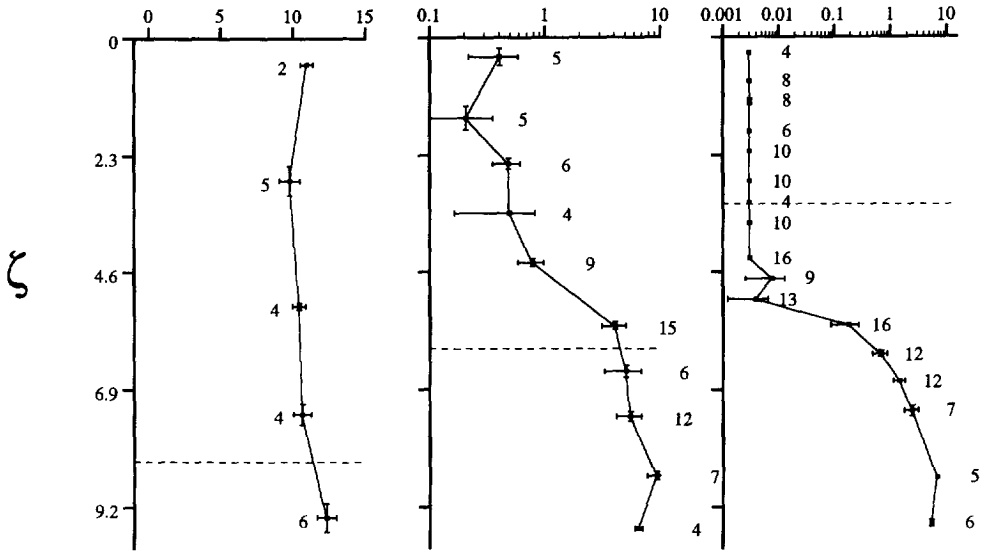
Fig. 1. Typical vertical profiles of density excess (σ_t) and *in situ* fluorescence. The dashed line indicates the bottom of the euphotic zone (Z_e), i.e. where PAR is 1% of the surface value. The eutrophic, mesotrophic and oligotrophic stations were located at 20°32N 18°35W, 18°30N 21°02W and 21°02N 31°08W, respectively.

collected at dawn using 10-l GoFlo bottles fixed on a Kevlar[®] wire were used for *in situ* primary production measurements (JGOFS protocol, 1994). Midday and dusk samples were collected using a rosette sampler with 12-l Niskin bottles equipped with silicone washers, and analyzed for nutrient and pigment concentrations. Micromolar $\text{NO}_2 + \text{NO}_3$ and PO_4 concentrations were determined using a Technicon Autoanalyzer[®] using methods of Wood *et al.* (1967) and Murphy and Ryley (1962), respectively. Nanomolar determinations of NO_2 and NO_3 concentrations were performed also using a Technicon Autoanalyzer[®], following the method of Raimbault *et al.* (1990). Vertical profiles of temperature, salinity and chl *a* fluorescence were measured using a CTD (SBE911plus, SEA-BIRD Electronics Inc.) and an *in situ* fluorometer (FL3000, Sea Tech Inc.).

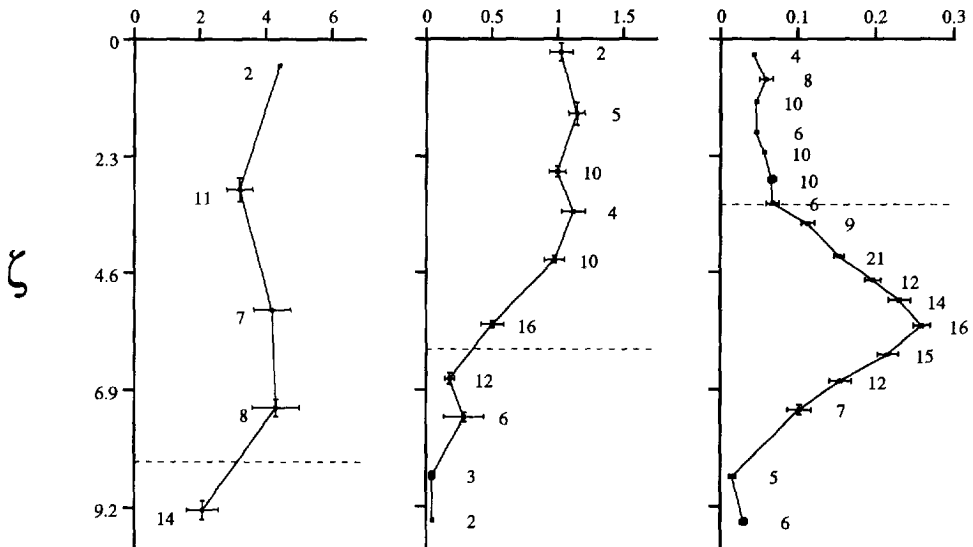
Discrete sample pigment concentrations were determined using fluorometry, spectrofluorometry, and HPLC. In all cases, filtration was performed using glass fiber filters (Whatman GF/F). Fluorometric determination of chl *a* + pheopigment concentration was performed as described by Parsons *et al.* (1984) using 100% methanol (rather than acetone) and extraction duration of 0.5 h. Spectrofluorometric determination of

EUTROPHIC MESOTROPHIC OLIGOTROPIC

NO₂+NO₃ (μM)



Chl concentration (mg m⁻³)



chlorophylls was carried out onboard using the method of Neveux and Lantoine (1993). Samples for liposoluble pigment analysis were stored in liquid nitrogen immediately following filtration and later measured by HPLC after extraction in 100% methanol at a shore-base laboratory as described by Claustre and Marty (1995). The HPLC system allowed a separation of divinyl-*chl a* (DV-*chl a*) and *chl a* sufficiently well resolved to quantify both concentrations using the peak heights. The extinction coefficient used for DV-*chl a* was 105.61 g^{-1} (Morel *et al.*, 1993). All three pigment analysis methods provided similar vertical patterns for total *chl a* (*chl a* and DV-*chl a*; hereafter denoted Chl), yet fluorometric and spectrofluorometric measurements always led to values clearly above those obtained by HPLC. As a rule, interpretation was based on HPLC results. When HPLC data were missing, spectrofluorometric (or fluorometric) measurements were used; they were "converted into HPLC data" by using conversion factors (calculated from samples for which all methods were simultaneously applied). A "non-photosynthetic pigment index" (NPP index) was computed from the HPLC analyses as the ratio (weight : weight) of non-photosynthetic pigments to which photoprotection is often ascribed (i.e. zeaxanthin plus diatoxanthin, diadinoxanthin and β -carotene) to total pigments (i.e. non-photosynthetic, chlorophylls and photosynthetic carotenoids; Bidigare *et al.*, 1990).

Daily measurements of submarine PAR (400–700 nm), performed using a custom-built quantum meter, were used to calculate optical depth (ζ) at each station as:

$$\zeta = K_d z$$

where K_d is the vertical attenuation coefficient for downward PAR irradiance (m^{-1}) and z is the depth (m); ζ is used to scale Figs 2–8. The euphotic layer, Z_e , operationally defined as the depth of 1% surface PAR irradiance, corresponds to $\zeta = 4.6$.

In vivo absorption measurements of suspended particles were performed using 1–9 l of seawater filtered onto 25 mm Whatman GF/F glass-fiber filters under low vacuum pressure. Wet filters were placed between a light source (tungsten lamp) and the entrance to an integrating sphere connected by an optic fiber to a LI-1800UW Licor irradiance meter. Transmitted light was measured between 350 and 750 nm with 1-nm resolution. The baseline was measured prior to filtration using the same filter soaked for 1 h in filtered seawater. Absorption was also measured after pigment extraction, in order to determine the spectral absorption due to unpigmented detrital particles. Pigments were extracted by immersion of the filter in a small volume of methanol (Kishino *et al.*, 1985, 1986). Particles were not washed from the filter. Both spectra (total particulate matter and non-algal matter) were corrected for the pathlength amplification (" β ") effect according to Bricaud and Stramski (1990). Algal absorption was calculated by subtracting detrital from total particle absorption (Kishino method) or by using the numerical decomposition technique of Bricaud and Stramski (1990). Both methods lead to convergent results when applied to the same sample. Spectral absorption coefficients [$a(\lambda)$] were normalized to the sum of Chl and pheopigments (when present) contents to derive algal Chl-specific spectral absorption

Fig. 2. Mean vertical (optical depth, ζ) distribution of $\text{NO}_2 + \text{NO}_3$ concentration and *chl a* + DV-*chl a* (Chl) concentrations. For the mesotrophic and oligotrophic sites, $\text{NO}_2 + \text{NO}_3$ concentration is plotted on a log scale. When undetectable, $\text{NO}_2 + \text{NO}_3$ concentration is given the detection threshold value (3 nM). The dashed line indicates the bottom of the surface mixed-layer and the euphotic depth is at $\zeta = 4.6$. The number of samples at each depth is indicated beside each data point. The error bars indicate \pm the standard error.

coefficients [$a_{\text{ph}}^*(\lambda)$]. These values were convoluted (according to equation (2)) with the spectral composition of light delivered by the lamp (in the incubator) or by the flash tube (FRR fluorometer) to provide the appropriate \bar{a}^* values.

The P^{B} vs E curves were determined using a radial photosynthetron (described in Babin *et al.*, 1994). Each seawater sample was dispensed into twelve 50-ml subsamples in polystyrene tissue culture flasks inoculated with 2–12 μCi of $\text{H}^{14}\text{CO}_3^-$ and stacked within an irradiance gradient in front of a 250W arc lamp (OSRAM, HQI-T 250 W/D). All samples were exposed to a PAR ranging from *ca* 15 to 550 $\mu\text{mol quanta m}^{-2} \text{s}^{-1}$, except those collected near the surface at the OLIGO site, which were exposed to *ca* 25–900 $\mu\text{mol quanta m}^{-2} \text{s}^{-1}$. Samples from 10 depths were simultaneously incubated for 60–120 min; each sample was maintained at a temperature reproducing the *in situ* temperature (at $\pm 1^\circ\text{C}$).

The Chl-specific initial slope (α^{B}) and saturation level ($P^{\text{B}}_{\text{max}}$) of the P^{B} vs E curves were derived by fitting to experimental data points a hyperbolic tangent function (Jassby and Platt, 1976) with a variable intercept, using the Quasi-Newton algorithm of Systat[®] statistical package. Photoinhibition was generally observed at high irradiances for samples collected below the euphotic zone at the OLIGO site. The corresponding points were excluded from the curve-fitting procedure.

For determinations of f , 50–100 ml samples from discrete depths were dark adapted for 30 min. Fluorescence flash yields were measured in duplicate subsamples with a deck-based FRR fluorometer (described in Greene *et al.*, 1994; Vassiliev *et al.*, 1994 and Falkowski and Kolber, 1995). Briefly, in the FRR method, PS2 reaction centers are rapidly closed by a train of 5- μs flashlits that cumulatively saturate the photochemical reaction. The rate of closure of reaction centers is used to derive the effective absorption cross-section of PS2 by fitting the following expression on fluorescence and energy measurements:

$$F_i = F_o + F_v \left[1 - \exp \left(-\sigma_{\text{PS2}} \sum_{j=0}^{i-1} I_j \right) \right] \quad (5)$$

where F_i is the fluorescence flash yield recorded following the i th flash, F_o is the fluorescence flash yield prior to the FRR protocol, F_v is the maximum variable fluorescence, i.e. ($F_m - F_o$), and I_j is the energy of the j th flash in the burst train of flashes. The average of 20 sets of measurements on each sample were used to calculate F_o , F_m and σ_{PS2} . The average coefficient of variation for the measurements was $< 2\%$ on an individual sample, and $< 5\%$ on replicate samples from the same station and depth.

The spectral output of the arc lamp used in the radial photosynthetron was determined using a spectroradiometer (LI-COR LI-1800UW) equipped with a cosine collector fixed at the end of a 2-m optic-fiber (see Babin *et al.*, 1994). The spectral composition of the xenon flash tube used in the FRR fluorometer was derived from the manufacturers data (EG&G) and spectral absorption characteristics of the blocking filters (see Kolber and Falkowski, 1993). The incubator source includes all PAR wavelengths, whereas the FRR flash source has a restricted spectrum centered on 440 nm with half-maximum width of 70 nm. These differences must be accounted for before comparisons between α^{B} and σ_{PS2} can be made. For example, a change in the absorption maximum wavelength between different phytoplankton populations without a necessary change in the absorption amplitude will alter σ_{PS2} . To correct for spectral difference in experimental lamps, measured values of α^{B} and σ_{PS2} were normalized for an ideal "white" spectrum [i.e. with $E(\lambda)$ assumed to be constant from 400 to 700 nm]. This normalization was made using:

$$\alpha^B(\text{white}) = \alpha^B(\text{exp}) \frac{\bar{a}^*(\text{white})}{\bar{a}^*(\text{incubator})} \quad (6a)$$

and

$$\sigma_{\text{PS2}}(\text{white}) = \sigma_{\text{PS2}}(\text{exp}) \frac{\bar{a}^*(\text{white})}{\bar{a}^*(\text{FRR})} \quad (6b)$$

where the subscript "white" refers to values for hypothetical white illumination and "exp" refers to experimental values measured on the actual sources (lamp or flash tube). Discussion below is based on $\alpha^B(\text{white})$ and $\sigma_{\text{PS2}}(\text{white})$, even if $\alpha^B(\text{exp})$ or $\sigma_{\text{PS2}}(\text{exp})$ are used without normalization when calculating $\phi_{\text{C max}}$ (equation (1)) or the ratio of σ_{PS2} to $\bar{a}^*(\text{FRR})$ (equation (7) and Fig. 10 later on).

RESULTS

Diel and day-to-day variability in vertical profiles of all measured variables were small compared to site-to-site differences. Therefore, the following site-to-site comparison is made using mean profiles computed for all variables measured at each of the three sites.

While we make no assumption about the identity of the specific limiting nutrient, we note that the addition of $4 \mu\text{M NO}_3^-$ stimulated phytoplankton growth at the oligotrophic site in simulated *in situ* incubations (Falkowski and Kolber, 1995). We also note that nitrate : phosphate ratios were highly stable at all sites. Hence we simply reference nutrient limitation to the nitrogen concentration ($\text{NO}_2 + \text{NO}_3$).

Eutrophic site

The EUtrophic (EU) site, located about 130 km off the Mauritanian coast, was in a permanent, nutrient-rich, upwelling area supporting a large phytoplankton community. $\text{NO}_2 + \text{NO}_3$ concentrations were $> 10 \mu\text{M}$ in the surface layer (Fig. 2), and Chl was uniformly distributed within the 40 m upper mixed-layer (Fig. 1) with an average concentration of about 4 mg m^{-3} (Fig. 2). Pheopigment concentrations were on average 30% of total Chl + pheo concentration. Mean euphotic depth (Z_e) was 17 m. Pigment composition revealed a clear dominance of chl *c*-containing phytoplankton species, mostly diatoms (Claustre, 1994). *In vivo* Chl-specific absorption spectra (Fig. 3) are also typical of diatoms (Prézelin and Boczar, 1986), with low $a_{\text{ph}}^*(\lambda)$ values, which indicate large pigment packaging. Ratios of $\alpha^B(\text{exp})/\alpha^B(\text{white})$ and $\sigma_{\text{PS2}}(\text{exp})/\sigma_{\text{PS2}}(\text{white})$ were constant with depth, averaging 0.9 and 1.73, respectively. The NPP index was < 0.05 at all depths (Fig. 4). α^B and P_{max}^B were nearly constant with depth (Fig. 5). Therefore E_k , the irradiance at which photosynthesis starts to saturate [with $E_k = P_{\text{max}}^B/\alpha^B(\text{white})$], was also constant. The maximum quantum yield $\phi_{\text{C max}}$ (~ 0.05), computed using equation (1) with a constant \bar{a}^* value of $0.011 \text{ m}^2 (\text{mg Chl})^{-1}$, and f were also nearly constant with depth (Figs 7 and 8). It should be noted, that replicated samples obtained in the upper 10 m during midday at this site had dark-adapted variable fluorescence values 30–40% lower than those at 20 m depth. The depression in variable fluorescence was abolished at dawn. The midday depression is indicative of photoinhibitory damage to PS2 reaction centers (Long *et al.*, 1994).

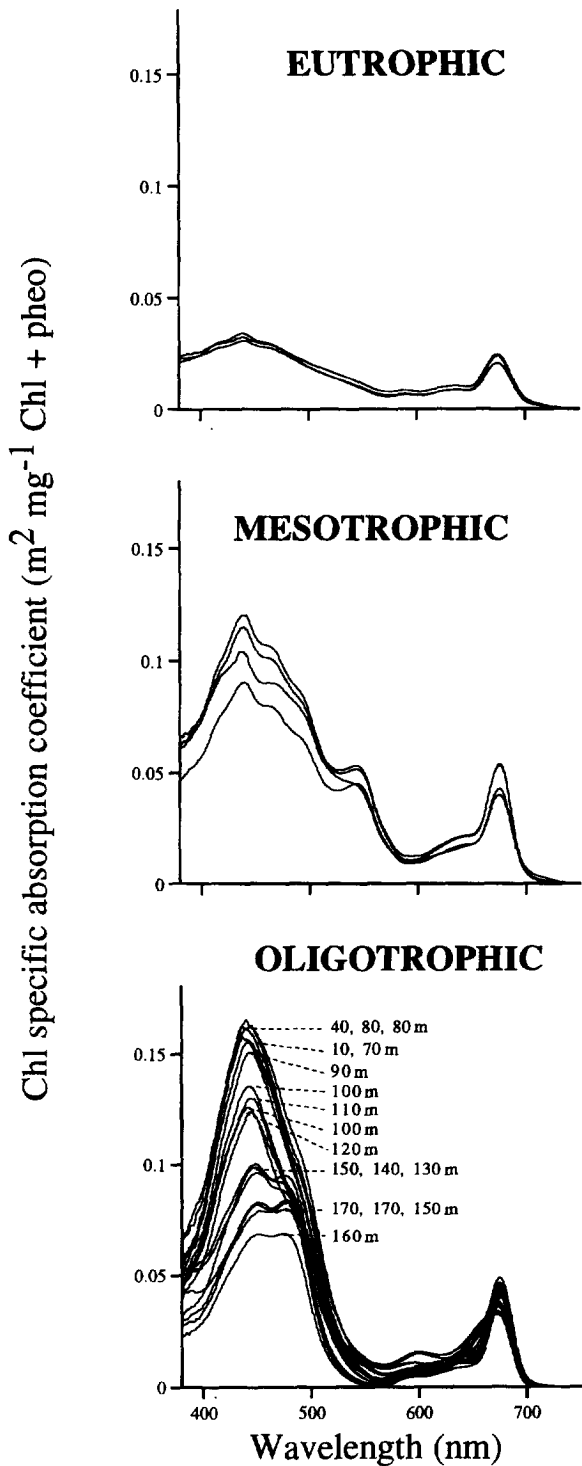


Fig. 3. Spectral values of the Chl specific absorption coefficient at different depths.

EUTROPHIC MESOTROPHIC OLIGOTROPHIC

NPP index

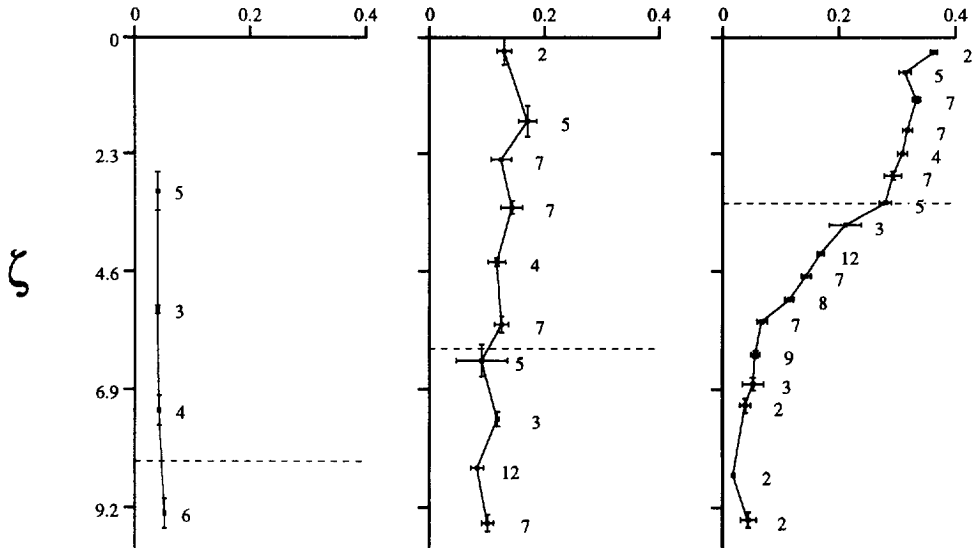


Fig. 4. Mean vertical (optical depth, ζ) profiles of the NPP index. The dashed line indicates the bottom of the surface mixed layer. The error bars indicate \pm the standard error.

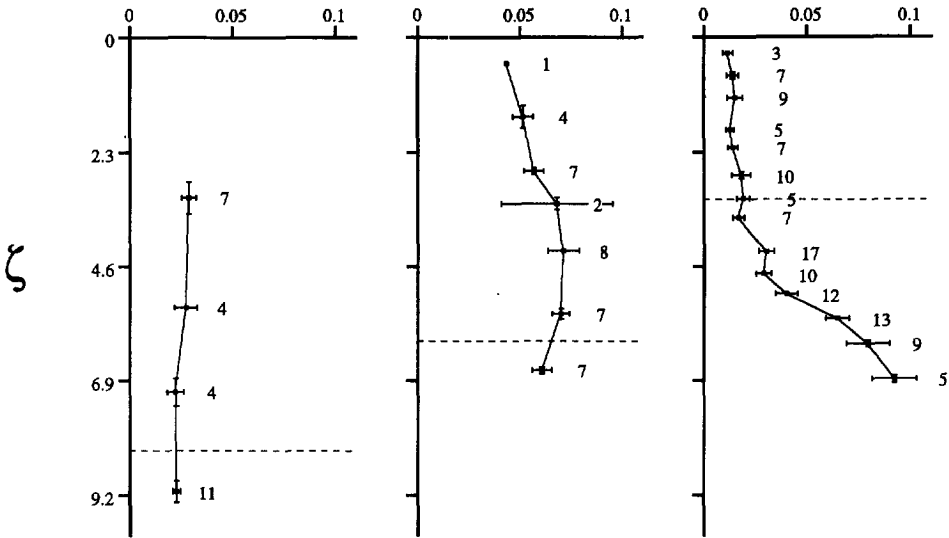
Mesotrophic site

The mesotrophic (MESO) site, located 400 km offshore and at the edge of the Mauritanian upwelling zone, was remotely influenced by advected nutrient-rich waters. $\text{NO}_2 + \text{NO}_3$ concentration averaged $0.5 \mu\text{M}$ within the mixed layer (Fig. 2), Chl concentrations were roughly constant ($\sim 1 \text{ mg m}^{-3}$) throughout the euphotic layer, before decreasing at $\zeta > 5.5$ (Figs 1 and 2), and pheopigments were undetectable. The absorption band of phycoerythrin at 548 nm (Fig. 3) and flow cytometric measurements using red and orange fluorescence (Partensky *et al.*, 1996) both indicated a predominance of cyanobacteria. Significant concentrations of chl *c* and fucoxanthin indicated that diatoms also contributed to algal biomass. The NPP index averaged 0.12, although this ratio may be overestimated because the HPLC protocol used could not differentiate zeaxanthin from lutein, the main light-harvesting carotenoid of chl *b*-containing species; the ratio of chl *b* to Chl averaged 0.2. Variability in the shape and amplitude of the $a_{\text{ph}}^*(\lambda)$ spectrum was not statistically significant and therefore a constant \bar{a}^* [$0.0452 \text{ m}^2 (\text{mg Chl})^{-1}$] was used for $\phi_{\text{C max}}$ calculations. Ratios of $\alpha^{\text{B}}(\text{exp})/\alpha^{\text{B}}(\text{white})$ and $\sigma_{\text{PS2}}(\text{exp})/\sigma_{\text{PS2}}(\text{white})$ were 0.92 and 1.88, respectively.

The α^{B} slope (Fig. 5) increased slightly from the surface down to $\zeta = 4.6$ while $P_{\text{max}}^{\text{B}}$ remained fairly constant at $8 \text{ mg C} (\text{mg Chl})^{-1} \text{ h}^{-1}$. Consequently, E_k decreased smoothly with depth (Fig. 5). Both $\phi_{\text{C max}}$ and f increased slightly with depth (Figs 7 and 8). As at the EU site, the near surface samples had lower f -values at midday, but these were fully

EUTROPHIC MESOTROPHIC OLIGOTROPHIC

α^B [mg C (mg Chl)⁻¹ h⁻¹(μ mol quanta m⁻² s⁻¹)⁻¹]



P^B_{max} [mg C (mg Chl)⁻¹ h⁻¹]

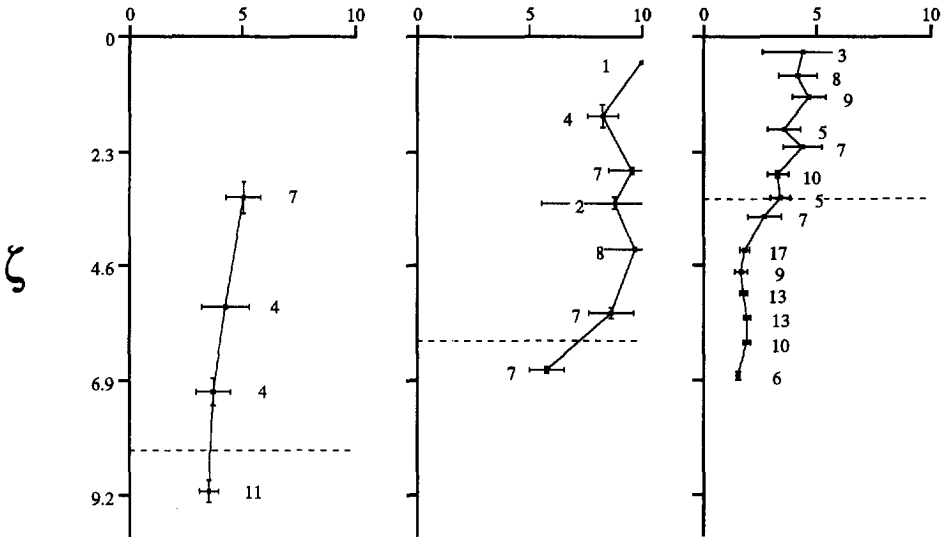


Fig. 5. Mean vertical (optical depth, ζ) profiles of the initial slope of the P^B vs E curve (α^B), the maximum rate of carbon fixation (P^B_{max}) and the saturation irradiance (E_k). The error bars indicate \pm the standard error.

EUTROPHIC MESOTROPHIC OLIGOTROPHIC

$$E_k (\mu\text{mol quanta m}^{-2} \text{s}^{-1})$$

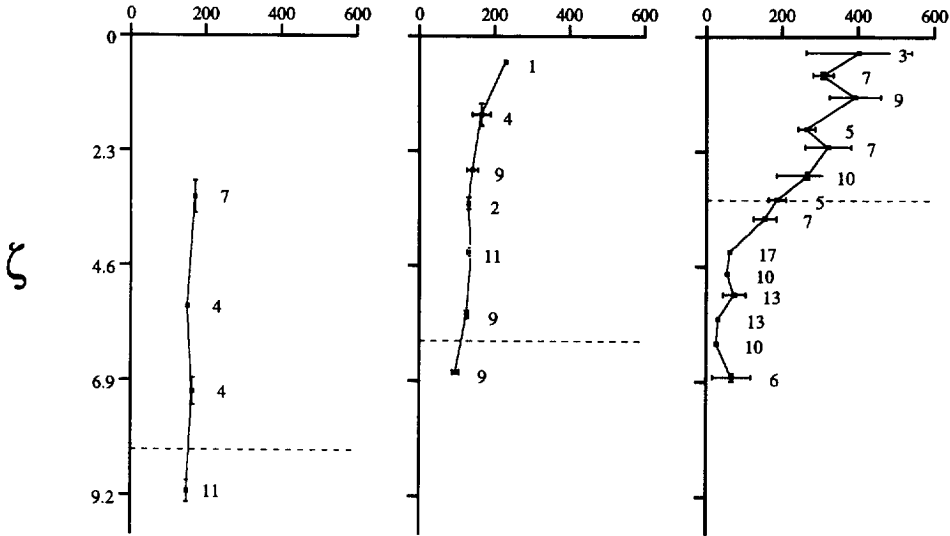


Fig. 5. *Continued.*

recovered before sunrise. Except for the deepest and the near surface samples, σ_{PS2} was essentially constant with depth (Fig. 8).

Oligotrophic site

The oligotrophic (OLIGO) site was located 1400 km offshore in the North Atlantic gyre. The mixed-layer depth averaged about 70 m, but varied by as much as 20 m over the 10 days spent at this site. The euphotic depth averaged *ca* 105 m and covaried with mixed-layer depth. The variation in physical mixed-layer depth, resulting from internal wave effects, was partly removed from the physiological responses by normalizing data to optical depths. At this site, $\text{NO}_2 + \text{NO}_3$ was undetectable (detection threshold = 3 nM) in the mixed layer, and Chl concentrations were extremely low, averaging *ca* 0.05 mg m^{-3} (Figs 1 and 2). A nutricline developed between 100 and 120 m with $\text{NO}_2 + \text{NO}_3$ increasing to *ca* $9 \mu\text{M}$ below ~ 120 m, and a deep Chl maximum (DCM) developed with Chl concentration reaching $0.25\text{--}0.30 \text{ mg m}^{-3}$. Pheopigments were undetectable throughout the whole water column.

HPLC analysis of the phytoplankton pigment composition revealed a vertical segregation of phytoplankton species (see the detailed analysis of Claustre and Marty, 1995). In the surface mixed layer, the high NPP index (Fig. 4) was mainly due to a high zeaxanthin concentration shared by cyanobacteria and prochlorophytes. Cyanobacteria were dominant in this upper layer, as the DV-chl *a* to Chl ratio was only 0.28. Within the DCM (between $\zeta = 4$ and 5), prochlorophytes became dominant with a DV-chl *a* to Chl ratio reaching 0.5. The NPP index decreased in the water column in a gradual way throughout the mixed layer, and abruptly below (Fig. 4). Additionally, the sum of 19'

hexanoyloxyfucoxanthin and 19'butanoyloxyfucoxanthin (19'HF + 19'BF) to Chl within the DCM was 0.38 (these pigments are typical of small chl *c*-containing picoeukaryotes; see Hooks *et al.*, 1988). From the DCM to $\zeta = 10$ (i.e. the 0.01% light depth), picoeukaryotes were progressively more abundant as evidenced by the ratio of (19'HF + 19'BF) to Chl increasing to 0.53 and a ratio of DV-chl *a* to Chl decreasing to 0.38. A similar vertical distribution of algal species was observed by Morel *et al.* (1993) at the same location during a previous cruise (EUMELI no. 3; October 1991). In the mixed layer, the $a_{ph}^*(\lambda)$ values between 400 and 500 nm were particularly high (Fig. 3) because of high zeaxanthin to Chl ratios. Within the DCM and below, the $a_{ph}^*(\lambda)$ values were notably diminishing at blue wavelengths and additional absorption bands of DV-chl *b* (prochlorophytes) appeared around 480 and 650 nm. These results are consistent with the observation of an increase in the ratio of DV-chl *b* to Chl, from 0.08 in the mixed layer up to 0.64 within the DCM. On the upper shoulder of the DCM (100–120 m), intermediate $a_{ph}^*(\lambda)$ spectral patterns were observed, in correspondence with moderate contributions of zeaxanthin and DV-chl *b*.

Depth dependent variations in $a_{ph}^*(\lambda)$ were accounted for when computing $\phi_{C\max}$ for the OLIGO site. Absorption spectra were not always measured coincidentally with samples for P^B vs E and FRR determinations. When plotted as a function of ζ , the pooled OLIGO \bar{a}^* values (pertinent to incubator and FRR experiments) form a regular pattern (Fig. 6); this pattern was fitted by a hyperbolic tangent function in order to interpolate the value for each sample at the needed optical depth. The same procedure was applied to the ratio $\bar{a}^*(FRR)/\bar{a}^*(white)$, which is depth-dependent (Fig. 6), whereas the ratio $\bar{a}^*(incubator)/\bar{a}^*(white)$ remains practically constant (0.78) with depth (not shown).

From the top to the bottom in the mixed layer, α^B increased slightly, P_{\max}^B decreased slightly, whereas E_k was halved (from *ca* 400 to 200 $\mu\text{mol quanta m}^{-2} \text{s}^{-1}$; Fig. 5). Below the mixed layer, α^B increased sharply (maximum at $\zeta = 7$) and P_{\max}^B and E_k decreased slightly. The vertical profile of $\phi_{C\max}$ is similar to that of α^B . Within the upper mixed layer, $\phi_{C\max}$ increased slightly [average = 0.007 mol C (mol quanta) $^{-1}$] and between $\zeta = 3.5$ and 7 it increased up to 0.063 mol C (mol quanta) $^{-1}$ (Fig. 7). At mid-day, f showed a depression for the upper 1.5 to 2 optical depths, and then increased gradually from the surface to the deep Chl maximum (Fig. 8). Variable fluorescence decreased for the deepest samples. The near-surface depression in fluorescence yields was virtually abolished in predawn samples (data not shown), while the low deep values were invariant throughout the day. On average, the f -values in the mixed layer were 50–60% lower than those found at the EU site. Throughout the water column, σ_{PS2} increased slightly, but regularly.

DISCUSSION

Intersite differences

The EUMELI sites were selected to compare the photophysiological responses of the phytoplankton in three distinctly differing oceanographic regimes with respect to nutrient availability, euphotic zone and mixed-layer depths, and phytoplankton biomass and species composition.

At the eutrophic site, the mixed layer was twice as deep as the euphotic zone depth and nutrients were abundant. A diatom-dominated algal community, with vertically uniform pigment concentration and constant photophysiological responses (α^B , P_{\max}^B , $a_{ph}^*(\lambda)$, $\phi_{C\max}$, f), extended throughout the mixed layer. The MESO site was similar to the EU site

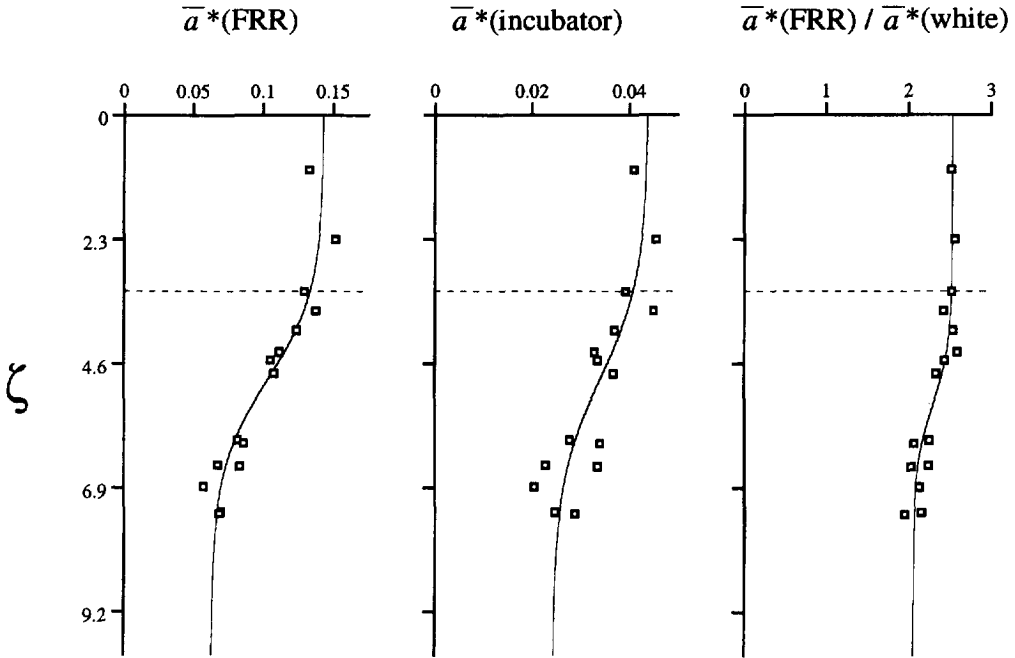


Fig. 6. Vertical distribution of $\bar{a}^*(\text{FRR})$, $\bar{a}^*(\text{incubator})$ and the ratio $\bar{a}^*(\text{FRR})/\bar{a}^*(\text{white})$ at the oligotrophic site (see text). The dashed line indicates the bottom of the surface mixed layer. Solid lines represent the corresponding non-linear regression equations: $\bar{a}^*(\text{FRR}) = -0.04 \tanh[0.6(\zeta - 4.9)] - 0.1$ ($R^2 = 0.94$), $\bar{a}^*(\text{incubator}) = -0.00098 \tanh[0.52(\zeta - 4.9)] - 0.034$ ($R^2 = 0.74$), and $\bar{a}^*(\text{FRR}) / \bar{a}^*(\text{white}) = -0.235 \tanh[0.91(\zeta - 5.36)] - 2.32$ ($R^2 = 0.85$).

in that the mixed layer also extended beyond the euphotic zone, although the nutrient concentrations and chlorophyll biomass (dominated by cyanobacteria) were much lower. Physiological parameters were essentially constant even if some vertical trends can be detected, indicating that a slight photoacclimation could have occurred within the not fully homogenized algal community. The \bar{a}^* coefficients were higher than at the EU site (by a factor of 3), and the relative proportion of non-photosynthetic pigments was noticeably increased (Figs 3 and 4).

The oligotrophic site was dramatically different from the other two sites. Euphotic depth (110 m) extended beyond the mixed-layer depth (70 m), giving rise to two physically segregated algal communities. Nutrient-limited cells living in the upper mixed layer were adapted to high irradiance conditions as indicated by high P_{max}^B , E_k and NPP index values. A low-light-adapted algal community existed in the stratified deep layers, forming a deep Chl maximum, supported by higher nutrient levels. Both communities were dominated by picoplankton, but with different species composition (Claustre and Marty, 1995). Physiological parameters were essentially constant within the upper mixed layer. Photoadaptive trends were detected, however, such as the slight decrease in P_{max}^B , E_k , or the NPP index, which denotes that vertical mixing was not actively developed. Below the surface mixed layer, strong gradients occurred in α^B , $a_{\text{ph}}^*(\lambda)$ and $\phi_{\text{C max}}$. Distinct changes in f and σ_{PS2} were also apparent within the pycnocline.

EUTROPHIC MESOTROPHIC OLIGOTROPHIC

$\phi_{C \max}$ (mol C mol⁻¹ quanta)

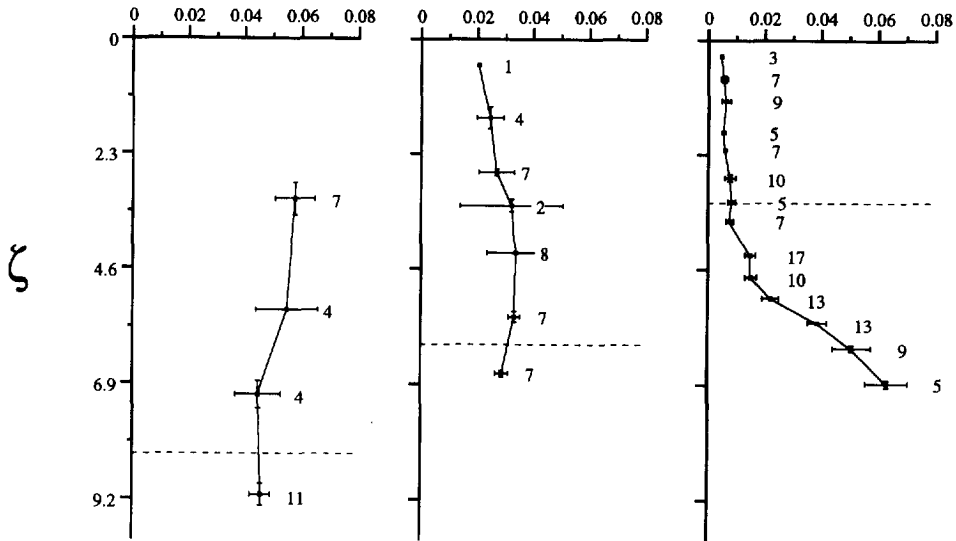


Fig. 7. Mean vertical (optical depth; ζ) profiles of the maximum quantum yield of carbon fixation ($\phi_{C \max}$). The dashed line indicates the bottom of the surface mixed layer. The error bars indicate \pm the standard error.

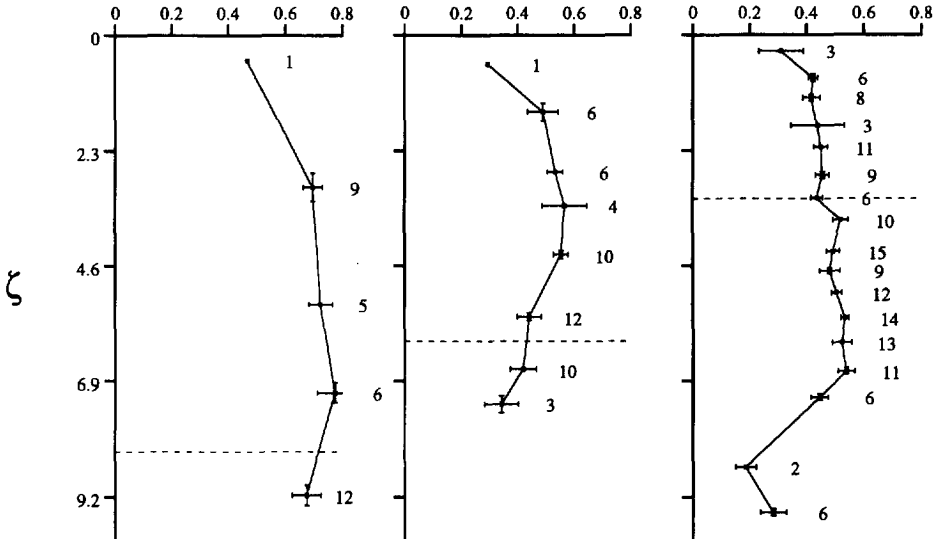
Natural extent of $\phi_{C \max}$ variability

Several attempts have been made to derive the maximum quantum yield of carbon fixation in marine environments. The first estimates were based on *in situ* measurements of ¹⁴C uptake and were limited to those samples incubated at depths close to Z_e so that irradiance is less than E_k , and a direct estimation of α^B becomes possible (reviewed by Bannister and Weidemann, 1984). Historically, variability in $\phi_{C \max}$ was inferred from α^B estimates by assuming a constant \bar{a}^* , derived from the literature. From measurements able to discriminate between living and detrital particle absorption (Kishino *et al.*, 1985, 1986) obtained more accurate values of $\phi_{C \max}$ (ranging from 0.02 to 0.1 mol C (mol quanta)⁻¹). These estimates, however, were also limited to *in situ* data at the base of the euphotic zone.

Cleveland *et al.* (1989) reported the first depth profiles of $\phi_{C \max}$ by measuring both α^B and \bar{a}^* simultaneously. A 3-fold change in $\phi_{C \max}$ [0.033–0.102 mol C (mol quanta)⁻¹] occurred within their 14 values determined along two vertical profiles in the northwestern Sargasso Sea. Lower $\phi_{C \max}$ values and wider ranges of variation were then reported by Schofield *et al.* (1993) in the southern California Bight [from 0.016 to 0.059 mol C (mol quanta)⁻¹], by Marra and Bidigare (1994) in the northwest Atlantic [from 0.005 to 0.065 mol C (mol quanta)⁻¹] and by Lizotte and Priscu (1994) in Antarctic ice-covered lakes [from 0.0015 to 0.051 mol C (mol quanta)⁻¹]. Recently, Babin *et al.* (1995) monitored vertical and temporal variations in $\phi_{C \max}$ within the Estuary and Gulf of St Lawrence and

EUTROPHIC MESOTROPHIC OLIGOTROPHIC

f



σ_{PS2} (rel. units)

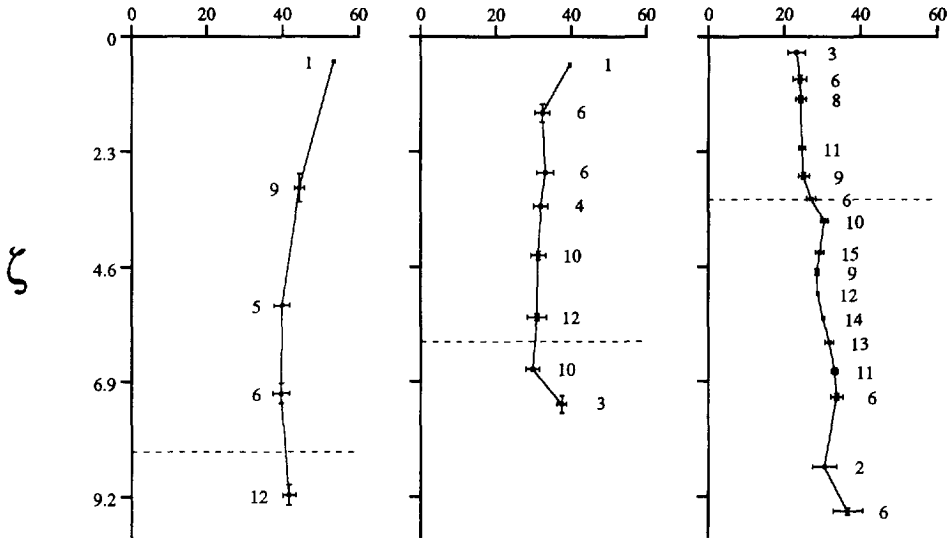


Fig. 8. Mean vertical (optical depth; ζ) profiles of the fraction of functional PS2 reaction centers (f) and the effective cross-section of PS2 (σ_{PS2}). The dashed line indicates the bottom of the surface mixed layer. The error bars indicate \pm the standard error.

observed a 20-fold change in $\phi_{C \max}$ [from 0.004 to 0.08 mol C (mol quanta)⁻¹] with clear diel variations.

In the present study, $\phi_{C \max}$ varied from 0.05 to 0.035 mol C (mol quanta)⁻¹ between the eutrophic and mesotrophic sites, respectively, with little depth dependence (Fig. 7). In contrast, both the lowest [0.005 mol C (mol quanta)⁻¹] and highest $\phi_{C \max}$ values [0.063 mol C (mol quanta)⁻¹] were observed at the oligotrophic site with a global range similar to those listed above.

Schofield *et al.* (1993) and Marra and Bidigare (1994) found no correlation between $\phi_{C \max}$ and environmental factors; Cleveland *et al.* (1989) and Lizotte and Priscu (1994), however, found a negative correlation with the distance from the nitracline; and Babin *et al.* (1995) inferred variations to NNP. During EUMELI, it was possible to discriminate between the influences of NO₂ + NO₃ concentration and of the NPP index on $\phi_{C \max}$, owing to the simultaneous measurements of f and σ_{PS2} provided by the FRR technique, and to detailed pigment analyses.

Relationship between $\phi_{C \max}$, f and nitrate availability

The dependence of $\phi_{C \max}$ on nitrate supply observed in the laboratory (Cleveland and Perry, 1987; Kolber *et al.*, 1988; Herzig and Falkowski, 1989) suggests that nutrients should play an important role in determining photosynthetic yields in nature (Welschmeyer and Lorenzen, 1981; Chalup and Laws, 1990). At sea, correlations with the distance to the nitracline, which may provide some indication about the nitrate supply, were reported by Cleveland *et al.* (1989) and Lizotte and Priscu (1994). A similar correlation was also suggested by Kolber *et al.* (1990) for the maximum quantum efficiency of photochemistry, ϕ_{PS2} . The data obtained from laboratory studies were based on the rate of supply of nutrient (i.e. chemostat cultures), not on the concentration of nutrient *per se*. However, to a first order, the flux of nutrients is related to their concentration within the euphotic zone, and a qualitative relationship between ϕ_{PS2} and nitrate concentration was described by Falkowski *et al.* (1991) and Geider *et al.* (1993).

The vertical profiles of f in the present study can be subdivided into three distinct segments (Fig. 8). (i) A surface depression was observed during mid-day, resulting from photodamage of reaction centers at supraoptimal irradiance (Baker and Bowyer, 1994; Falkowski *et al.*, 1994; Long *et al.*, 1994). The photoinhibited portion of the water column is restricted to the upper first optical depths and was found at all three sites. (ii) Below the photoinhibited portion, there is a part of the water column with intermediate or elevated values of photochemical activity. In the OLIGO site the f -values tended to increase slightly with depth. (iii) In stable stratified layers at the OLIGO site, a deep section characterized by a decrease in the quantum yield was found below the DCM. The loss of photochemical activity in this portion of the water column likely reflects senescence of the cells, and is found in all oceanographic regimes examined thus far (Falkowski, unpublished). Only the intermediate section of the profiles can be usefully examined to understand the effects of nutrient supply on photochemical energy conversion efficiency.

In the present study, any attempt to derive a relation between f or $\phi_{C \max}$ and the distance to the nitracline fails because no nitracline existed at the EU site and, in contrast, a strong nitracline existed at the MESO and OLIGO sites; but f as well as $\phi_{C \max}$ were essentially constant above this layer. Therefore, changes in f and $\phi_{C \max}$ were examined with respect to

$\text{NO}_2 + \text{NO}_3$ concentration. Let us note that the occurrence of such a strong nitracline and of undetectable nutrient concentration in the upper layer suggest that $\text{NO}_2 + \text{NO}_3$ flux was negligible above the pycnocline at the OLIGO site.

The f -values for the three sites are plotted against $\text{NO}_2 + \text{NO}_3$ concentration in Fig. 9a. The lowest f -values at each site correspond to samples that displayed signs of photoinhibition (black symbols). Disregarding these three values, f increased from 0.42 to 0.57 when $\text{NO}_2 + \text{NO}_3$ concentration increased from undetectable levels to less than $1 \mu\text{M}$. A distinct increase in f (up to 0.8) was found between the MESO and EU sites. If it is assumed that nitrate availability is the sole factor affecting f , it induced a 2-fold variation.

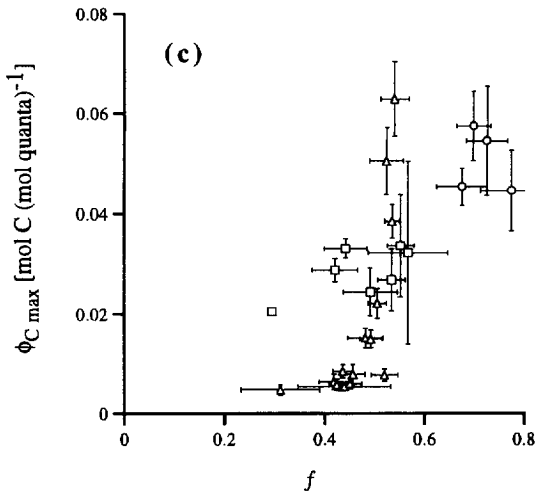
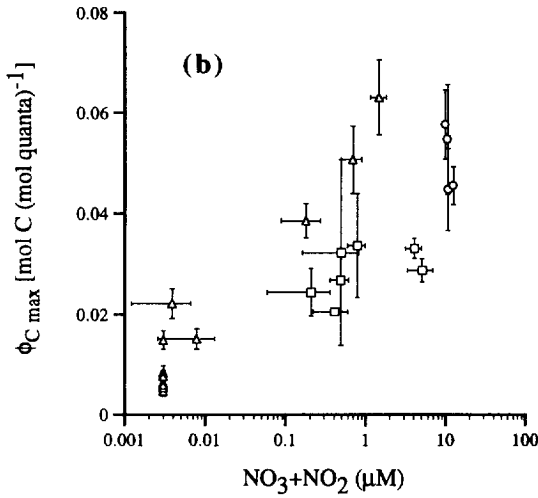
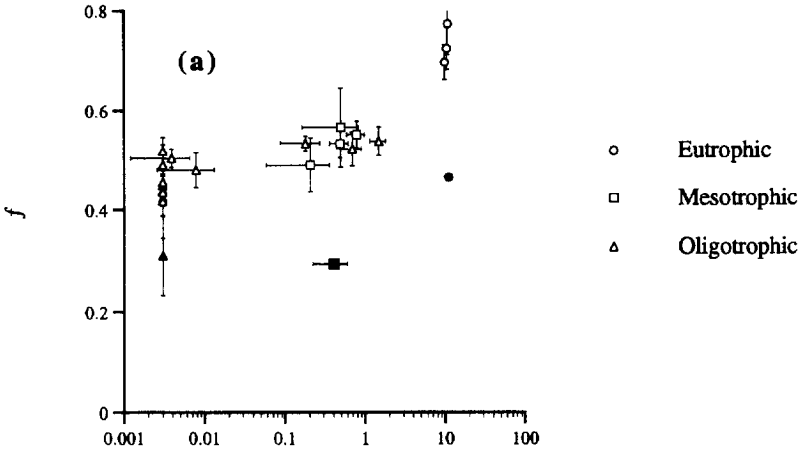
Theoretically, all factors affecting f should equally affect $\phi_{\text{C max}}$ (see equation (4)). The variations in $\phi_{\text{C max}}$ and in f , however, are not of the same amplitude (Figs 7 and 8) and the pattern in Fig. 9b, where $\phi_{\text{C max}}$ is plotted against $\text{NO}_2 + \text{NO}_3$ concentration, differs strongly from that in Fig. 9a. Note that no clear sign of photodamage appears on any of the $\phi_{\text{C max}}$ vertical profiles. The technique used to determine P_B vs E curves, which lasts a few hours between water collection and the end of incubations, may allow adequate time for recovery from surface photodamage.

In Fig. 9c, $\phi_{\text{C max}}$ and f are compared for the three sites. This figure tends to show that a rough covariation exists between these two yields, in spite of a large difference in their respective range of variation. Such a difference suggests that factors other than nitrogen can alter $\phi_{\text{C max}}$ without affecting f . The lack of linearity between the two yields variations lies in the fundamental difference in the processes they describe. $\phi_{\text{C max}}$ provides the bulk efficiency by which photons absorbed by all algal components are used to fix carbon. Photon capture and energy utilization can be described by the following three steps: (i) a fraction of the photons absorbed by the various algal pigments (in fact the whole algal matter) reaches chl a antenna (of both PS2 and PS1); (ii) a fraction of the photons reaching the chl a antenna leads to charge separation at the level of the reaction center; and (iii) a fraction of the electrons produced by light reactions is utilized for CO_2 reduction. These three steps are explicitly represented in equation (4), by a photon transfer efficiency term ($\sigma_{\text{PS2}} n_{\text{PS2}} / \bar{a}^*$), a functional term (f), and the photosynthetic quotient (R), respectively.

It should be noted that variable fluorescence measurements proceed from the basis of photons absorbed by PS2 reaction centers; i.e. if excitation energy is absorbed but does not lead to a photochemical electron transfer in PS2, no changes in fluorescence will be observed within the $150 \mu\text{s}$ of exposure to the FRR flashes. The fluorescence analysis requires no assumptions about \bar{a}^* , but conversely does not account for photons that are absorbed by the cell and are not used in linear electron transport.

Effect of non-photosynthetic pigments on $\phi_{\text{C max}}$

The photosynthetic quotient can vary only between 1 and $1.4 \text{ mol O}_2 (\text{mol C})^{-1}$ (Laws, 1991), and is never far from the second value in the marine environment. Therefore, the variation in R [in equation (4)] cannot be at the origin of the divergence between $\phi_{\text{C max}}$ and f evolutions. The variations in transfer efficiency are more likely responsible for the larger variation in $\phi_{\text{C max}}$, compared to that in f . Photosynthetically active pigments transfer absorbed photons to chl a within the antenna at an efficiency approaching 100% (reviewed by Fork and Mohanty, 1986 and Govindjee and Satoh, 1986). The role of dissipative, non-photosynthetic, pigments in altering the transfer efficiency is to be examined. This working



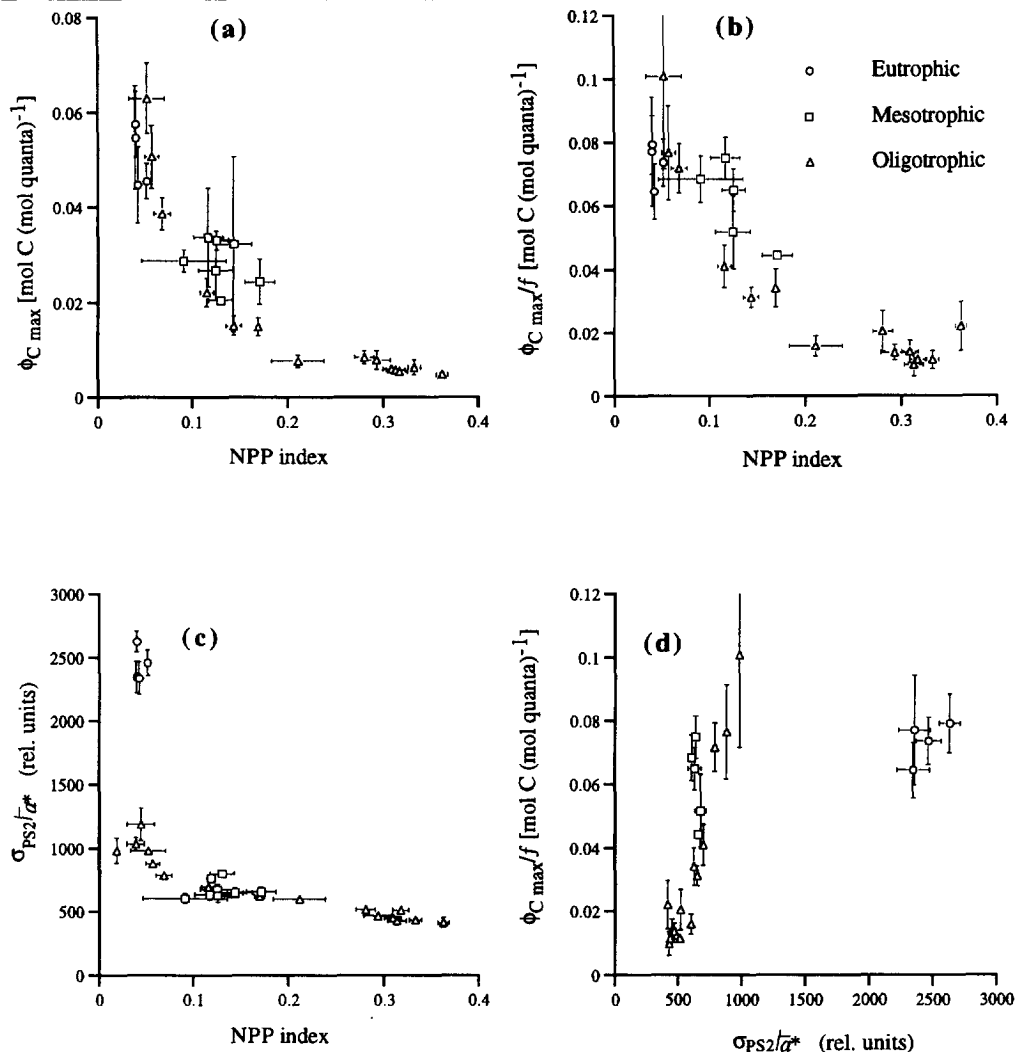


Fig. 10. Plot of (a) $\phi_{C \max}$, (b) $\phi_{C \max}/f$ and (c) $\sigma_{PS2}/\bar{\alpha}^*$ as a function of the non-photosynthetic pigment (NPP) index. The bottom panel (d) shows $\phi_{C \max}/f$ as a function of $\sigma_{PS2}/\bar{\alpha}^*$.

hypothesis is supported by the regular decrease of $\phi_{C \max}$ when plotted as a function of the NPP index (Fig. 10a).

The "xanthophyll cycle" is a prominent mechanism for photoprotection among plant species (Demmig-Adams, 1990; Demmig-Adams and Adams, 1992). In this system, zeaxanthin acts as an active photoprotectant pigment, probably by de-exciting the singlet state of chl *a*, made possible by the close physical association of zeaxanthin molecules with chl *a* molecules. The high turnover of the xanthophyll cycle allows a rapid (~ 2 min)

Fig. 9. Plot of (a) $\phi_{C \max}$ and (b) f , vs $\text{NO}_2 + \text{NO}_3$ concentration (log scale). When undetectable, $\text{NO}_2 + \text{NO}_3$ concentration is given the detection threshold value (3 nM). The bottom panel (c) shows $\phi_{C \max}$ as a function of f . Black symbols in panel (a) correspond to the surface sample of each site. The data points corresponding to the deep depression of f (ascribed in text to senescence) are not plotted.

production of zeaxanthin when light conditions exceed E_k . In most eukaryotic chl-*c* containing algae, diatoxanthin would play a role analogous to that of zeaxanthin (e.g. Olaizola and Yamamoto, 1994). Whilst zeaxanthin is an important photoprotectant in eukaryotic plant cells, prokaryotes (dominant at the OLIGO site) lack the accessory molecules required for a functional xanthophyll cycle (Partensky *et al.*, 1993). Furthermore, zeaxanthin molecules are associated with the cell wall rather than antenna chl *a* in cyanobacteria (Omata and Murata, 1983) and perhaps also in prochlorophytes (F. Partensky, personal communication, 1994). Though zeaxanthin appears to have no direct photoprotective role in prokaryotes (Kana *et al.*, 1988), Bidigare *et al.* (1989) nevertheless observed a spectrally dependent decrease in $\phi_{C \max}$ in the *Synechococcus* clone WH7803 at wavelengths corresponding to the zeaxanthin absorption maximum. The presence of any absorbing substance that enhances \bar{a}^* but does not lead to additional photosynthesis, entails a proportionate decrease of $\phi_{C \max}$, while α^B remains unchanged. Such "useless" absorption (neither leading to photosynthesis nor to photoprotective de-excitation) is the main effect of non-photosynthetic pigments on $\phi_{C \max}$ to be considered for prokaryotes.

Measured values of $\phi_{C \max}$ are highly correlated to the NPP index, and systematically depressed when the non-photosynthetic pigments proportion increases (Fig. 10a–b). From equation (4), the photon transfer efficiency can be isolated and expressed as:

$$\sigma_{PS2} n_{PS2} / \bar{a}^* = \frac{\phi_{C \max}}{f} R \quad (7)$$

Assuming a roughly stable R (see above), the variability in the transfer efficiency is reflected by change in the ratio $\phi_{C \max} / f$, which decreased with increasing NPP index (Fig. 10b). Assuming a relatively constant value of n_{PS2} (the total number of PS2 per unit chl *a*) a regular variation of σ_{PS2} / \bar{a}^* along with the NPP index can be identified for results from the OLIGO and MESO sites, but not for the EU site (Fig. 10c). For this site, the σ_{PS2} / \bar{a}^* values stand apart, as perhaps a consequence of an increase in the PS2 size (i.e. $1/n_{PS2}$) by a factor of 2. Figure 10d (as well as Fig. 10c) is shown to illustrate the variability in n_{PS2} .

The relative contribution of non-photosynthetic pigments to phytoplankton absorption [$c_{np}(\lambda)$] can be quantified using the following expression:

$$c_{np}(\lambda) = \frac{\sum_{m=1}^{np} \langle m \rangle a_m(\lambda)}{\sum_{m=1}^{all} \langle m \rangle a_m(\lambda)} \quad (8a)$$

where $a_m^*(\lambda)$ is the weight-specific absorption coefficient of the m th pigment in solvent and $\langle m \rangle$ is the concentration of this m th pigment. The numerator represents the sum of absorption by non-photosynthetic pigments, while the denominator is the sum of all pigments absorption. The spectral values of Chl-specific absorption by only photosynthetically active pigments, denoted $a_{act}^*(\lambda)$, is derived from $a_{ph}^*(\lambda)$, the measured Chl-specific absorption coefficient of algae, through:

$$a_{act}(\lambda) = a_{ph}(\lambda)[1 - c_{np}(\lambda)] \quad (8b)$$

To apply equations (8a) and (8b), absorption spectra of pigments in solvent were obtained from different laboratory phytoplankton cultures (using a photodiode array detector connected on the HPLC line). To reproduce *in vivo* absorption, wavelength shifts were applied to each pigment absorption spectrum (see Table 1). Figure 11 shows such a decomposition (using equations (8a) and (8b)) of a $a_{ph}^*(\lambda)$ spectrum, measured near surface

Table 1. Wavelength of maximum in vivo absorption (λ_{\max}), pigment weight-specific absorption coefficient at λ_{\max} [$a^*(\lambda_{\max})$] and pigment concentration used to compute the contribution of non-photosynthetic pigments in total phytoplankton absorption (equations (8a), (8b), Fig. 11). Pigment concentrations were measured on a sample collected at the surface (0 m) at the oligotrophic site (pheopigments were absent). Values of λ_{\max} were obtained from absorption measurements in solvent, wavelength shifted according to Bidigare et al. (1990). Only shifts in the blue part of the spectrum were considered as, over 550 nm, non-photosynthetic pigments have no contribution in phytoplankton absorption (see equation (8b)). Values of $a^*(\lambda_{\max})$ were also set according to Bidigare et al. (1990). For pigments not considered by them, we applied the wavelength shift and attributed the $a^*(\lambda_{\max})$ value of the closest pigment in terms of the spectral shape of absorption (as clustered in the table)

Pigment	λ_{\max} (nm)	$a^*(\lambda_{\max})$ ($\text{m}^2 \text{mg}^{-1}$)	Concentration ($\mu\text{g m}^{-3}$)
Chlorophyll <i>a</i>	440*	0.0265*	29
Divinyl-chlorophyll <i>a</i>	448	0.0265	12
Chlorophyll $c_1 + c_2$	460*	0.0708*	3
Fucoxanthin	491*	0.0368*	4
19'HF	488	0.0368	11
19'BF	486	0.0368	4
Peridinin	485	0.0368	1
β -Carotene†	462*	0.0603*	2
Zeaxanthin†	462	0.0603	30
Diadinoxanthin†	457	0.0603	6
α -Carotene	457	0.0603	2

*According to Bidigare *et al.* (1990).

†Non-photosynthetic pigment.

at the OLIGO site and when the NPP index is maximal. In this case, the spectrally integrated \bar{a}_{ph}^* is about 3 times larger than \bar{a}_{act}^* (both computed using equation (2)). Therefore, considering that when the NPP index is close to zero, \bar{a}_{act}^* is strictly equal to \bar{a}_{ph}^* , a 3-fold increase in $\phi_{\text{C max}}$ is to be expected at the OLIGO site, from the upper to the lower levels, or as well, from the OLIGO (surface layer) to the EU site (all layers). Note that this range corresponds to the one observed for $\sigma_{\text{PS2}}/\bar{a}^*$ for the MESO and OLIGO sites (400–1200).

First-order determinant of $\phi_{\text{C max}}$ variations and the light–nutrient interaction

Cleveland *et al.* (1989) and Lizotte and Priscu (1994) on one hand, and Babin *et al.* (1995) on the other hand, respectively suspected effects of nitrogen and NPP on $\phi_{\text{C max}}$. However, their interpretations were based solely on correlation techniques. Deconvolution of the effects of different environmental factors is largely impeded by the fortuitous covariability often occurring between them at sea. At the OLIGO site, for instance (see Figs 2 and 4), the NPP index is high near the surface, where nitrate is absent, and close to zero at depth where nutrient is available. In the present study, the relationships between $\phi_{\text{C max}}$ and nitrogen or NPP were shown to be causal, using independent approaches (carbon uptake measurements, FRR fluorometry and pigments determinations). Nitrate and NPP were found to be first-order determinant of $\phi_{\text{C max}}$ variations. The determination of f allowed

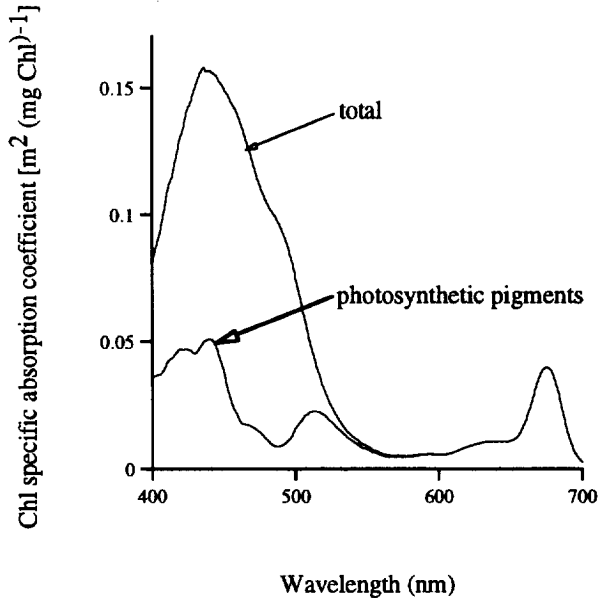


Fig. 11. Example of partitioning in spectral values of the *in vivo* Chl specific absorption coefficient, between total and photosynthetic phytoplankton pigments (see equations (8a) and (8b)).

association of a 2-fold variation in $\phi_{C \max}$ with nitrate availability. Non-photosynthetic pigments were found to be responsible for a 3-fold change in $\phi_{C \max}$. The concurrent effects of these independent factors upon $\phi_{C \max}$ could account for variations by a factor of 6. The causes of the remaining 2-fold variation in $\phi_{C \max}$ cannot be identified, even if the photosynthetic quotient and cyclic electron flow around PS1 can be set forth. Cyclic electron flow around PS1 can reduce $\phi_{C \max}$ and is “invisible” to FRR fluorescence methods. The cycle is related to the ratio of PS2:PS1 reaction centers. In diatoms, the ratio is generally > 1 , whilst in cyanobacteria it is generally < 0.25 . In prochlorophytes it is close to unity. Photons absorbed by PS1 may facilitate photochemical electron transfers independent of CO_2 fixation or O_2 evolution (and generate ATP in the process). Cyclic electron flow around PS1 conserves energy but is not “counted” in a photon budget for carbon assimilation. When cyanobacteria are limited by dissolved inorganic nitrogen, the loss of PS2 photochemical activity is not mirrored by a loss of photochemical activity in PS1 (Berges *et al.*, 1996).

In addition to being a first-order determinant, nutrients may also play an indirect role in $\phi_{C \max}$ variations. For instance, nutrient limitation has been found to affect the ability of phytoplanktonic cells to repair photodamaged reaction centers, and thus to favor photoinhibition (reviewed by Falkowski *et al.*, 1994). Herzig and Falkowski (1989) observed a gradual decrease in the cellular content of light harvesting pigments and gradual increase in the chlorophyll-specific absorption coefficient of algae with decreasing nitrate supply. Kolber *et al.* (1988) and Greene *et al.* (1992) observed a nearly systematic increase in the effective absorption cross-section of PS2 (σ_{PS2}) under nitrate and iron limitation, respectively. Moreover, nutrient limitation can lead to large changes in the production of NPP (in fact, nutrient limitation is used in commercial production schemes to enhance the production of carotenoids in microalgal mass culture). Hence, variations in nutrient supply induce modifications in light absorption, energy transfer, and

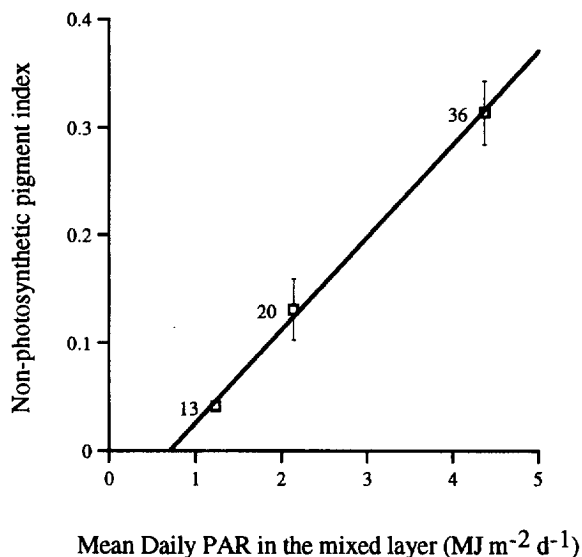


Fig. 12. Relationship between the daily PAR and the NPP index averaged for the upper mixed layer at the 3 EUMELI sites. The photosynthetically available radiation just beneath surface integrated over the day [$\overline{\text{PAR}}(0^-)$] was obtained from continuous deck measurements of the total downward irradiance converted into "PAR just beneath surface" by multiplying by 0.43 and assuming a 4% sea surface reflection.

photochemical charge separation in marine phytoplankton. Such an indirect role of nutrients in the ocean is hardly assessable. The present observations allow some remarks to be drawn about this issue.

The extent of photoinhibition depends, on one hand, on the rate of damage to reaction centers and, on the other hand, on the rate of repair of damaged reaction centers (Cullen and Neale, 1994; Long *et al.*, 1994). The former is a product of the effective absorption cross-section of the reaction center (normally PS2 is the site of damage; Prasil *et al.*, 1992), the incident PAR, and a quantum yield for damage. Repair is critically dependent upon the rate of supply of metabolic substrates, especially nucleic and amino acids (Prasil *et al.*, 1992). We observed the effects of photoinhibitory damage at all three sites, however, the repair mechanisms seemed to be able to mostly replace the damaged proteins within a day (there was full recovery of photochemical competence at night). There was evidence of incomplete repair at the OLIGO site (data not shown), however, in general we can conclude that the damage/repair balance was comparable between sites. Note that the high E_k values at the OLIGO site probably contribute to limiting the rate of damage. The steep surface depression in f observed near surface—obviously related to photoinhibition—was about the same at all sites (Fig. 8). Moreover, the occurrence of such a steep depression in all three cases indicates that photodamaged units were repaired before propagating down in the water column. So, it can be concluded that nutrient limitation controls photoinhibition neither near surface nor in the remainder of the mixed layer.

Rather than light, nutrient limitation may also be responsible for the high NPP index observed in the mixed layer at the OLIGO site. If the role of nutrient is difficult to assess, a clear view of how light actually controls the NPP index can be obtained by plotting the latter as a function of the mean daily PAR in the surface mixed layer ($\overline{\text{PAR}}_{Z_{\text{ml}}}$), computed as:

$$\overline{\text{PAR}}_{Z_{\text{ml}}} = \text{PAR}(0^-) \frac{[1 - e^{-4.5Z_{\text{ml}}/Z_e}]}{4.6Z_{\text{ml}}/Z_e} \quad (9)$$

where $\text{PAR}(0^-)$ is the total daily PAR just beneath surface, and Z_{ml} and Z_e are the depth of the mixed layer and euphotic zone, respectively. It can be seen that a tight relationship exists between the NPP index and $\overline{\text{PAR}}_{Z_{\text{ml}}}$ at the three sites (Fig. 12). It illustrates well how the combination between vertical mixing and light actually controlled phytoplankton photoacclimation (e.g. Cullen and Lewis, 1988) and supports the idea that the NPP development is mainly regulated by light availability.

CONCLUSIONS

The maximum quantum yield of carbon fixation varied by about 12-fold, from 0.005 to 0.063 mol C (mol quanta)⁻¹, in the natural phytoplankton community of the tropical northeast Atlantic. This range of variation was observed over three different sites representing typical eutrophic, mesotrophic and oligotrophic situations at tropical latitudes, and also at a single site (oligotrophic) between the upper layer and the deep chlorophyll maximum. The initial slope of the P^B vs E curve, α^B (corresponding to the product $\bar{a}^* \phi_{\text{C max}}$), varied 8-fold.

Two of the major sources of variation in $\phi_{\text{C max}}$ were clearly identified in this study: (i) the fraction of functional PS 2 reaction centers, f , led to a 2-fold variation in $\phi_{\text{C max}}$. The variations in f were largely brought about by nutrient limitation that affected the ability of cells to synthesize photochemical reaction centers. (ii) Variations in the light absorption contribution of non-photosynthetic pigments explained 3-fold variations in $\phi_{\text{C max}}$. The effect of f and NPP are multiplicative, and hence, their combined effect accounted for 6-fold variations in $\phi_{\text{C max}}$. The remaining 2-fold was not specifically identified; it could be related to variations in cyclic electron flow around PS1 or in the photosynthetic quotient. Although photoinhibition was not detected in $\phi_{\text{C max}}$ using a ¹⁴C technique, the steep surface depression in f observed at all sites suggests that photoinhibition actually affected $\phi_{\text{C max}}$ to the same extent *in situ*. These results establish that variations in $\phi_{\text{C max}}$ can be larger than those for \bar{a}^* , and that variability in both parameters must be considered independently in bio-optical models of primary production (see also Morel *et al.*, 1996).

Acknowledgements—This paper is an “EUMELI” contribution to the JGOFS-France Program. The first author received post-doctoral scholarships from the Fonds pour la Formation de Chercheurs et l’Aide à la Recherche (FCAR) of the Quebec Government, from the Université des Réseaux d’Expression Française/Association des Universités Partiellement ou Entièrement de Langue Française (UREF/AUPELF), and from the CEE program “Human Capital and Mobility” (contract CHRXCT 930312). P. G. Falkowski gratefully acknowledges support from CNRS and the John Simon Guggenheim Foundation. Additional support was provided by the U.S. Department of Energy under the contract DE-AC02-76CH00016 to BNL. We are grateful to D. Antoine for technical assistance for the photosynthesis-irradiance curve determinations, to P. Raimbault and F. Lantoin, who provided us with nutrient and spectrofluorometric pigment data, and to D. Tailliez and J. Raunet for CTD measurements. We express particular appreciation to M. Berhenfeld for his help and constructive criticism on initial versions of this work.

REFERENCES

- Babin M., A. Morel and A. Gagnon (1994) An incubator designed for extensive and sensitive measurements of phytoplankton photosynthetic parameters. *Limnology and Oceanography*, **39**, 496–510.

- Babin M., J.-C. Therriault, L. Legendre, B. Nieke, R. Reuter and A. Condal (1995) Relationship between the maximum quantum yield of carbon fixation and the minimum quantum yield of chlorophyll *a* *in vivo* fluorescence in the Gulf of St Lawrence. *Limnology and Oceanography*, **40**, 956–968.
- Baker N. K. and J. R. Bowyer (1994) *Photoinhibition of photosynthesis: from molecular mechanisms to the field*. Bios Scientific Publishers, Oxford, U.K.
- Bannister T. T. (1974) Production equations in terms of chlorophyll concentration, quantum yield and upper limit to production. *Limnology and Oceanography*, **19**, 1–12.
- Bannister T. T. (1979) Quantitative description of steady state, nutrient-saturated algal growth, including adaptation. *Limnology and Oceanography*, **24**, 76–96.
- Bannister T. T. and A. D. Weidemann (1984) The maximum quantum yield of phytoplankton photosynthesis *in situ*. *Journal of Plankton Research*, **6**, 275–294.
- Berges J. A., D. O. Charlebois, D. C. Mauzerall and P. G. Falkowski (1996) Differential effects of nitrogen limitation on photosynthetic efficiency of Photosystems I and II in microalgae. *Plant Physiology*, **110**, 689–696.
- Bigdare R. R., O. Schofield and B. B. Prézélin (1989) Influence of zeaxanthin on quantum yield of photosynthesis of *Synechococcus* clone WH7803 (DC2). *Marine Ecology Progress Series*, **56**, 177–188.
- Bigdare R. R., M. E. Ondrusek, J. H. Morrow and D. A. Kiefer (1990) *In vivo* absorption properties of algal pigments. *SPIE*, **1302**, 290–302.
- Bigdare R. R., B. B. Prézélin and R. C. Smith (1992) Bio-optical models and the problems of scaling. In: *Primary productivity and biogeochemical cycles in the sea*, P. G. Falkowski and A. D. Woodhead, editors, Plenum Press, New York, pp. 175–212.
- Bricaud A. and D. Stramski (1990) Spectral absorption coefficients of living phytoplankton and nonalgal biogenous matter: A comparison between the Peru upwelling area and Sargasso Sea. *Limnology and Oceanography*, **35**, 562–582.
- Butler W. L. (1978) Energy distribution in the photochemical apparatus of photosynthesis. *Annual Review of Plant Physiology*, **29**, 345–378.
- Butler W. L. and M. Kitajima (1975) Fluorescence quenching of in photosystem 2 of chloroplasts. *Biochimica et Biophysica Acta*, **376**, 116–125.
- Cha Y. and D. C. Mauzerall (1992) Energy-storage of linear and cyclic electron flows in photosynthesis. *Plant Physiology*, **100**, 1869–1877.
- Chalup M. S. and E. A. Laws (1990) A test of the assumptions and predictions of recent microalgal growth models with the marine phytoplankters *Pavlova Lutheri*. *Limnology and Oceanography*, **35**, 583–596.
- Claustre H. (1994) The trophic status of various oceanic provinces as revealed by phytoplankton pigment signatures. *Limnology and Oceanography*, **39**, 1207–1211.
- Claustre H. and J.-C. Marty (1995) Specific phytoplankton biomass and their relation to primary production in the tropical North Atlantic. *Deep-Sea Research I*, **42**, 1475–1493.
- Cleveland J. S. and M. J. Perry (1987) Quantum yield, relative specific absorption and fluorescence in nitrogen-limited *Chaetoceros gracilis*. *Marine Biology*, **94**, 489–497.
- Cleveland J. S., M. J. Perry, D. A. Kiefer and M. C. Talbot (1989) Maximal quantum yield of photosynthesis in the northwest Sargasso Sea. *Journal of Marine Research*, **47**, 869–886.
- Cullen J. J. and M. R. Lewis (1988) The kinetics of algal photoadaptation in the context of vertical mixing. *Journal of Plankton Research*, **10**, 1039–1063.
- Cullen J. J. and P. J. Neale (1994) Ultraviolet radiation, ozone depletion, and marine photosynthesis. *Photosynthesis Research*, **39**, 303–320.
- Demmig-Adams B. (1990) Carotenoids and photoprotection in plants: a role for the xanthophyll zeaxanthin. *Biochimica Biophysica Acta*, **1020**, 1–24.
- Demmig-Adams B. and W. W. Adams (1992) Photoprotection and other responses of plants to high light stress. *Annual Review of Plant Physiology and Plant Molecular Biology*, **43**, 599–626.
- Dubinsky Z. (1980) Light utilization efficiency in natural marine phytoplankton communities. In: *Primary productivity in the sea*, P. G. Falkowski, editor, Plenum, New York, pp. 83–98.
- Dubinsky Z. and T. Berman (1976) Light utilization efficiencies of phytoplankton in Lake Kinneret (Sea of Galilee). *Limnology and Oceanography*, **21**, 226–230.
- Dubinsky Z., P. G. Falkowski and K. Wyman (1986) Light harvesting and utilization by phytoplankton. *Plant Cell Physiology*, **27**, 1335–1349.
- Duysens L. N. M. and H. E. Sweers (1963) Mechanisms of the two photochemical reactions in algae as studied by

- means of fluorescence. In: *Studies on microalgae and photosynthetic bacteria*, University of Tokyo Press, Japan, pp. 353–372.
- Eppley R. W. and J. H. Sharp (1975) Photosynthetic measurements in the central North Pacific: The dark loss of carbon in 24-h measurements. *Limnology and Oceanography*, **20**, 981–987.
- Falkowski P. G. (1992) Molecular ecology of phytoplankton photosynthesis. In: *Primary productivity and biogeochemical cycles in the sea*, P. G. Falkowski and A. Woodhead, editors, Plenum Press, New York, pp. 47–67.
- Falkowski P. G. and Z. Kolber (1993) Estimation of phytoplankton photosynthesis by active fluorescence. *International Council for the Exploration of the Sea Symposium*, **197**, 92–103.
- Falkowski P. G. and Z. Kolber (1995) Variations in chlorophyll fluorescence yields in phytoplankton in the world oceans. *Australian Journal of Plant Physiology*, **22**, 341–355.
- Falkowski P. G. and J. A. Raven (in press) *Aquatic photosynthesis*, Blackwell, Oxford, U.K.
- Falkowski P. G., Y. Fujita, A. C. Ley and D. C. Mauzerall (1986a) Evidence for cyclic electron flow around photosystem II in *Chlorella pyrenoidosa*. *Plant Physiology*, **81**, 310–312.
- Falkowski P. G., K. Wyman, A. C. Ley and D. C. Mauzerall (1986b) Relationship of steady state photosynthesis to fluorescence in eucaryotic algae. *Biochimica Biophysica Acta*, **849**, 183–192.
- Falkowski P. G., A. Sukenik and R. Herzig (1989) Nitrogen limitation in *Isochrysis galbana* (Haptophyceae). II. Relative abundance of chloroplast proteins. *Journal of Phycology*, **25**, 471–478.
- Falkowski P. G., D. Ziemann, Z. Kolber and P. K. Bienfang (1991) Role of eddy pumping in enhancing primary production in the ocean. *Nature*, **352**, 55–58.
- Falkowski P. G., R. M. Greene and R. J. Geider (1992) Physiological limitations on phytoplankton productivity in the ocean. *Oceanography*, **5**, 84–91.
- Falkowski P. G., R. M. Greene and Z. Kolber (1994) Light utilization and photoinhibition of photosynthesis in marine phytoplankton. In: *Photoinhibition of photosynthesis: from molecular mechanisms to the field*, N. R. Baker and J. R. Bowyer, editors, Bios Scientific, Oxford, U.K., pp. 407–431.
- Fork D. C. and P. Mohanty (1986) Fluorescence and other characteristics of blue-green algae (Cyanobacteria), red algae, and cryptomonads. In: *Light emission by plant and bacteria*, Govindjee, J. Ames and D. C. Fork, editors, Academic Press, New York, p. 451–496.
- Geider R. J., R. M. Greene, Z. Kolber, H. L. McIntyre and P. G. Falkowski (1993) Fluorescence assessment of the maximum quantum efficiency of photosynthesis in the western North Atlantic. *Deep-Sea Research I*, **40**, 1205–1224.
- Govindjee and K. Satoh (1986) Fluorescence properties of chlorophyll *b*- and chlorophyll *c*-containing algae. In: *Light emission by plant and bacteria*, Govindjee, J. Ames and D. C. Fork, editors, Academic Press, New York, pp. 497–537.
- Greene R. M., R. J. Geider, Z. S. Kolber and P. G. Falkowski (1992) Iron-induced changes in light harvesting and photochemical energy conversion processes in eukaryotic algae. *Plant Physiology*, **100**, 565–575.
- Greene R. M., Z. S. Kolber, D. G. Swift, N. W. Tindale and P. G. Falkowski (1994) Physiological limitation of phytoplankton photosynthesis in the eastern equatorial Pacific determined from variability in the quantum yield of fluorescence. *Limnology and Oceanography*, **39**, 1061–1074.
- Haxo F. T. and L. R. Blinks (1950) Photosynthetic action spectra of marine algae. *Journal Genetic Physiology*, **33**, 389.
- Heber U., M. R. Kirk and N. K. Boardman (1979) Photoreactions of cytochrome *b*-559 and cyclic electron flow in photosystem II of intact chloroplasts. *Biochimica Biophysica Acta*, **546**, 292–306.
- Henley W. J., G. Levasseur, L. A. Franklin, S. T. Lindley, J. Ramus and C. B. Osmond (1992) Diurnal responses of photosynthesis and fluorescence in *Ulva rotunda*. *Marine Ecology Progress Series*, **75**, 19–28.
- Herzig R. and P. G. Falkowski (1989) Nitrogen limitation in *Isochrysis galbana* (haptophyceae). I. Photosynthetic energy conversion and growth efficiency. *Journal of Phycology*, **25**, 462–471.
- Hooks C. E., R. R. Bidigare, M. D. Keller and R. R. L. Guillard (1988) Coccolid eukaryotic marine ultraplankters with four different HPLC pigment signatures. *Journal of Phycology*, **24**, 571–580.
- Jassby A. D. and T. Platt (1976) The relationship between photosynthesis and light for natural assemblages of marine phytoplankton. *Journal of Marine Research*, **12**, 421–430.
- JGOFS protocol (1994) Protocols for the joint global ocean flux study (JGOFS) core measurements. *IOC Manual and Guides*, **29**, 170 pp.
- Kana T. M., P. M. Glibert, R. Goericke and N. A. Welschmeyer (1988) Zeaxanthin and β -carotene in *Synechococcus* WH7803 respond differently to irradiance. *Limnology and Oceanography*, **33**, 1623–1627.

- Kiefer D. A. and B. G. Mitchell (1983) A simple, steady state description of phytoplankton growth based on absorption cross section and quantum efficiency. *Limnology and Oceanography*, **28**, 770–776.
- Kiefer D. A., W. S. Chamberlain and C. R. Booth (1989) Natural fluorescence of chlorophyll *a*: Relationship to photosynthesis and chlorophyll concentration in the western South Pacific gyre. *Limnology and Oceanography*, **34**, 868–881.
- Kishino M., M. Takahashi, N. Okami and S. Ichimura (1985) Estimation of the spectral absorption coefficients of phytoplankton in the sea. *Bulletin of Marine Science*, **37**, 634–642.
- Kishino M., N. Okami, M. Takahashi and S. Ichimura (1986) Light utilization efficiency and quantum yield of phytoplankton in a thermally stratified sea. *Limnology and Oceanography*, **31**, 557–566.
- Kok B. (1960) Efficiency of photosynthesis. In: *Handbuch der Pflanzenphysiologie*, W. Ruhland, editor, Vol. 5, Part 1. Springer, Berlin, pp. 563–633.
- Kok B. and R. Radmer (1976) Energy requirements of a biosphere. In: *Chemical evolution*, C. Ponnampertuma, editors, Academic Press, New York, pp. 183–197.
- Kok B., B. Forbush and M. McGloin (1970) Cooperation of charges in photosynthetic oxygen evolution. I. A linear four step mechanism. *Photochemistry and Photobiology*, **11**, 453–475.
- Kolber Z. and P. G. Falkowski (1992) *Fast Repetition Rate (FRR) fluorometer for making in situ measurements of primary productivity*. Proceedings of Ocean 92 Conference, Newport, Rhode Island.
- Kolber Z. and P. G. Falkowski (1993) Use of active fluorescence to estimate phytoplankton photosynthesis *in situ*. *Limnology and Oceanography*, **38**, 1646–1665.
- Kolber Z., J. Zehr and P. G. Falkowski (1988) Effect of growth irradiance and nitrogen limitation on photosynthetic energy conversion in Photosystem II. *Plant Physiology*, **88**, 923–929.
- Kolber Z., K. D. Wyman and P. G. Falkowski (1990) Natural variability in photosynthesis energy conversion efficiency: A field study in the Gulf of Maine. *Limnology and Oceanography*, **35**, 72–79.
- Lavergne J. and E. Leci (1993) Properties of inactive photosystem 2 centers. *Photosynthesis Research*, **35**, 323–343.
- Lavergne J. and H. W. Trissl (1995) Theory of fluorescence induction in photosystem-2-derivation of analytical expressions in a model including exciton-radical-pair equilibrium and restricted energy-transfer between photosynthetic units. *Biophysical Journal*, **68**, 2474–2492.
- Laws E. A. (1991) Photosynthetic quotients, new production and net community production in the open ocean. *Deep-Sea Research*, **38**, 143–167.
- Ley A. C. and D. Mauzerall (1982) Absolute absorption cross sections for photosystem II and the minimum quantum requirement for photosynthesis in *Chlorella vulgaris*. *Biochimica Biophysica Acta*, **680**, 95–106.
- Li W. K. W. and J. C. Goldman (1981) Problems in estimating growth rates of marine phytoplankton from short-term ¹⁴C assays. *Microbial Ecology*, **7**, 113–121.
- Lizotte M. P. and J. C. Priscu (1994) Natural fluorescence and quantum yield in vertical stationary phytoplankton from perennially ice-covered lakes. *Limnology and Oceanography*, **39**, 1399–1410.
- Long S. P., S. Humpries and P. G. Falkowski (1994) Photoinhibition of photosynthesis in nature. *Annual Review of Plant Physiology and Plant Molecular Biology*, **45**, 655–662.
- Marra J. and R. R. Bidigare (1994) The question of a nutrient effect on the bio-optical properties of phytoplankton. *SPIE Ocean Optics XII*, **2258**, 152–162.
- Morel A. (1991) Light and marine photosynthesis: a spectral model with geochemical and climatological implications. *Progress in Oceanography*, **26**, 263–306.
- Morel A., Y.-H. Ahn, F. Partensky, D. Vaultot and H. Claustre (1993) *Prochlorococcus* and *Synechococcus*: A comparative study of their optical properties in relation to their size and pigmentation. *Journal of Marine Research*, **51**, 617–649.
- Morel A., D. Antoine, M. Babin and Y. Dandonneau (1996) Measured and modeled primary production in the northeast Atlantic (EUMELI JGOFS program): The impact of natural variations in photosynthetic parameters on model predictive skill. *Deep-Sea Research I*, **43**, 1273–1304.
- Murphy J. and J. B. Ryley (1962) A modified single solution method for determination of phosphate in natural waters. *Analytica Chimica Acta*, **27**, 31–36.
- Myers J. E. (1980) On the algae: Thoughts about physiology and measurements of efficiency. In: *Primary productivity in the sea*, P. G. Falkowski, editor, Plenum, New York, pp. 1–16.
- Myers J. E. (1987) Is there significant cyclic electron flow around photoreaction I in cyanobacteria?. *Photosynthesis Research*, **14**, 55–69.
- Neale P. J. (1987) Algal photoinhibition and photosynthesis in the aquatic environment. In: *Photoinhibition*, D. J. Kyle, C. B. Osmond and C. J. Arntzen, editors, Elsevier, Amsterdam, pp. 39–65.

- Neveux J. and F. Lantoine (1993) Spectrofluorometric assay of chlorophylls and pheopigments using least-square approximation technique. *Deep-Sea Research I*, **40**, 1747–1765.
- Odum E. P. (1971) *Fundamentals of ecology*, Saunders, Philadelphia, 574 pp.
- Olaizola M. and H. Y. Yamamoto (1994) Short-term response of the diadinoxanthin cycle and fluorescence yield to high irradiance in *Chaetoceros muelleri* Lemm. (Bacillariophyceae). *Journal of Phycology*, **30**, 606–612.
- Olaizola M., J. Laroche, Z. Kolber and P. G. Falkowski (1994) Non-photochemical fluorescence quenching and the diadinoxanthin cycle in a marine diatom. *Photosynthesis Research*, **41**, 357–370.
- Omata T. and N. Murata (1983) Isolation and characterization of the cytoplasmic membranes from the blue-green alga (cyanobacterium) *Anacystis nidulans*. *Plant Cell Physiology*, **24**, 1101–1112.
- Parsons T. R., Y. Maita, and C. M. Lalli (1984) *A manual of chemical and biological methods for seawater analysis*, Pergamon, Oxford, U.K., 173 pp.
- Partensky F., N. Hoepffner, W. K. W. Li, O. Ulloa and D. Vaultot (1993) Photoacclimation of *Prochlorococcus* sp. (Prochlorophyta) strains isolated from North Atlantic and Mediterranean Sea. *Plant Physiology*, **101**, 285–296.
- Partensky F., J. Blanchot, F. Lantoine, J. Neveux and D. Marie (1996) Vertical structure of picophytoplankton at different trophic sites of the tropical northeastern Atlantic Ocean. *Deep-Sea Research I*, **43**, 1191–1213.
- Platt T., C. L. Gallegos and W. G. Harrison (1980) Photoinhibition of photosynthesis in natural assemblage of marine phytoplankton. *Journal of Marine Research*, **38**, 687–701.
- Platt T., S. Sathyendranath, O. Ulloa, W. G. Harrison, N. Hoepffner and J. Goes (1992) Nutrient control of phytoplankton photosynthesis in the western North Atlantic. *Nature*, **356**, 229–231.
- Prasil O., N. Adir and I. Ohad (1992) Dynamics of photosystem II: Mechanism of photoinhibition and recovery processes. In: *The photosystems: Structure, function and molecular biology*, J. R. Barber, editor, Elsevier, Oxford, U.K., pp. 295–348.
- Prézelin B. B. and B. A. Boczar (1986) Molecular bases of cell absorption and fluorescence in phytoplankton: potential applications to studies in oceanography. In: *Progress in phycological research*, Vol. 4., F. T. Round and D. J. Chapman, editors, Biopress, Bristol, U.K., pp. 349–464.
- Raimbault P., P. Slawyk, B. Coste and J. Fry (1990) Feasibility of using an automatic procedure for the determination of seawater nitrate in the 0–100 nM range: examples from field and culture. *Marine Biology*, **104**, 347–351.
- Sakshaug E., K. Anderson and D. A. Kiefer (1989) A steady state description of growth and light absorption in the marine planktonic diatom *Skeletonema costatum*. *Limnology and Oceanography*, **34**, 198–205.
- Schofield O., B. B. Prézelin, R. R. Bidigare and R. C. Smith (1993) *In situ* photosynthetic quantum yield. Correspondence to hydrographic and optical variability within the Southern California Bight. *Marine Ecology Progress Series*, **93**, 25–37.
- Slovacek R. E., D. Crowther and G. Hind (1980) Relative activities of linear and cyclic electron flows during chloroplast CO-fixation. *Biochimica Biophysica Acta*, **592**, 495–505.
- Smith R. C., B. B. Prézelin, R. R. Bidigare and K. S. Baker (1989) Bio-optical modeling of photosynthetic production in coastal waters. *Limnology and Oceanography*, **34**, 1524–1544.
- Vassiliev I. R., O. Prasil, K. D. Wyman, Z. Kolber, A. K. Hanson Jr, J. E. Prentice and P. G. Falkowski (1994) Inhibition of PSII photochemistry by PAR and UV radiation in natural phytoplankton communities. *Photosynthesis Research*, **42**, 61–64.
- Welschmeyer N. A. and C. J. Lorenzen (1981) Chlorophyll-specific photosynthesis and quantum yield efficiency at subsaturating light intensities. *Journal of Phycology*, **17**, 283–293.
- Wood E. P. K., F. A. J. Armstrong and F. A. Richards (1967) Determination of nitrate in seawater by cadmium copper reduction to nitrite. *Journal of the Marine Biology Association of United Kingdom*, **47**, 23–31.

APPENDIX I

The terms used to describe fluorescence yields and their derivative products are sometimes confusing, and we (Falkowski and Kolber) have used two different notations for expressing the fraction of functional PS2 reaction centers. We will clarify the issues here.

It can be shown (Butler, 1978) that the maximum quantum efficiency (ϕ_{PS2}) of photochemistry in PS2 is given by the following relation:

$$\phi_{\text{PS2}} = \frac{F_m - F_o}{F_m} = \frac{F_v}{F_m} \quad (\text{A1})$$

where F_o is the normal fluorescence flash yield observed when all traps are open in the dark and F_m is the maximal flash yield obtained when all traps are closed (e.g. in the presence of DCMU, or following exposure to a saturating, single-turnover flash). The maximum measured value of PS2 in microalgae is *ca* 0.75, but that is atypical. A more typical maximum value is *ca* 0.65, and is remarkably independent of growth irradiance if cells are grown in nutrient-replete conditions and are not photoinhibited.

When assaying the fraction of closed or open PS2 reaction centers, at any given time, it is convenient to normalize the change in fluorescence to F_o . We have described the relationship:

$$\Delta\phi_{\text{SAT}} = \frac{F_m - F_o}{F_o} = \frac{F_v}{F_o} = \frac{F_m}{F_o} - 1 \quad (\text{A2})$$

This is a so-called Stern–Volmer representation of fluorescence quenching, and is related to ϕ_{PS2} by a hyperbolic function [$\phi_{\text{PS2}} = \Delta\phi_{\text{SAT}} / (1 - \Delta\phi_{\text{SAT}})$]. The maximum value of $\Delta\phi_{\text{SAT}}$ is *ca* 1.8 (corresponding to a $\phi_{\text{PS2}} = 0.65$). Hence, we assumed that if all PS2 reaction centers are open and “functional”, $\Delta\phi_{\text{SAT}} \approx 1.8$. $\Delta\phi_{\text{SAT}}$ is more linearly related to O_2 evolving centers than ϕ_{PS2} (Falkowski *et al.*, 1986b), although use of either will generally agree throughout most of the functional region of the fluorescence responses we observe in the sea.

The use of $\Delta\phi_{\text{SAT}}$ to derive f is supported by theoretical arguments (Lavergne and Trissl, 1995), as well as experimental data (Kolber *et al.*, 1988). The model implicitly assumes that energy can be transferred between PS2 reaction centers (Lavergne and Trissl, 1995). That energy transfer between PS2 reaction centers occurs in natural phytoplankton is certain.

APPENDIX II

NOTATION

Symbol	Significance	Units
Chl	Sum of DV-chl <i>a</i> and chl <i>a</i> concentrations	mg m ⁻³
λ	Wavelength	nm
\bar{a}^*	Mean absorption coefficient of algae weighted by the irradiance spectrum	m ² (mg Chl + pheo) ⁻¹
$a_{\text{ph}}^*(\lambda)$	chl <i>a</i> -specific absorption coefficient of algae	m ² (mg Chl + pheo) ⁻¹
$E(\lambda)$	Scalar irradiance	μmol quanta m ⁻² s ⁻¹
PAR	Photosynthetically available radiation	μmol quanta m ⁻² s ⁻¹
α^{B}	Chlorophyll-specific initial slope of the P^{B} vs E curve	mg C (mg Chl) ⁻¹ (mol available quanta m ⁻²) ⁻¹
$P_{\text{max}}^{\text{B}}$	Maximum rate of carbon fixation per unit Chl	mg C (mg Chl) ⁻¹ h ⁻¹
E_k	Irradiance at which carbon fixation begins to saturate	μmol quanta m ⁻² s ⁻¹
$\Phi_{\text{C max}}$	Maximum quantum yield of photosynthetic carbon fixation	mol C (mol quanta) ⁻¹
F_o	<i>In vivo</i> fluorescence flash yield induced by a weak probe flash	Rel. units
F_m	<i>In vivo</i> fluorescence flash yield induced by a weak probe flash and following a saturating flash	Rel. units
f	Fraction of reaction centers that remains functional	Dimensionless
ϕ_{PS2}	Maximum quantum efficiency of photochemistry	Dimensionless
σ_{PS2}	Effective absorption cross-section of PS2	m ² (quanta) ⁻¹
n_{PS2}	Total number (functional and non-functional) of PS2 per unit of chl <i>a</i>	mol electron (mg Chl) ⁻¹
ϕ_e	Quantum yield of electron transport for O_2 evolution (assumed to be 0.25)	mol O_2 (mol electron) ⁻¹
R	Photosynthetic quotient	mol O_2 (mol C) ⁻¹
K_d	Vertical attenuation coefficient for downward PAR irradiance	m ⁻¹

Symbol	Significance	Units
ζ	Optical depth	Dimensionless
$c_{np}(\lambda)$	Contribution of non-photosynthetic pigments to phytoplankton absorption	Dimensionless
a^*_m	Weight-specific absorption coefficient of the m th pigment in solvent	$\text{m}^2 \text{mg}^{-1}$
$\langle m \rangle$	Concentration of the m th pigment	$\mu\text{g m}^{-3}$
$a^*_{act}(\lambda)$	Spectral values of Chl-specific absorption coefficient of photosynthetically active pigments	$\text{m}^2 (\text{mg chl } a)^{-1}$
$\overline{\text{PAR}}_{Z_{ml}}$	Mean daily PAR in the surface mixed layer	$\text{MJ m}^{-2} \text{day}^{-1}$
$\text{PAR}(0^-)$	Total daily PAR just beneath surface	$\text{MJ m}^{-2} \text{day}^{-1}$
Z_{ml}	Depth of the mixed layer	m
Z_e	Depth of the euphotic zone	m
$\alpha^B(n)$	$n = \text{exp}$: experimental value of α^B $n = \text{white}$: value of α^B estimated for white illumination conditions	
$\sigma_{PS2}(n)$	$n = \text{exp}$: experimental value of σ_{PS2} $n = \text{white}$: value of σ_{PS2} estimated for white illumination conditions	
$\bar{a}^*(n)$	$n = \text{FRR}$: value of \bar{a}^* obtained for the the FRR fluorometer $n = \text{incubator}$: value of \bar{a}^* obtained for the incubator $n = \text{white}$: value of \bar{a}^* computed for white illumination conditions	